# Understanding the abnormal brain activity in epilepsy as a potential predictor of the onset of an epileptic seizure

J. M. Dunn[1] R. A. J. Masterton[2] D. F. Abbott[3]
R. S. Anderssen[4]

(Received 6 November 2010; revised 21 March 2011)

**Abstract**

The Brain Research Institute (BRI) uses various types of indirect measurements, including EEG and fMRI, to understand and assess brain activity and function. As well as the recovery of generic information about brain function, research also focuses on the utilisation of such data and understanding to study the initiation, dynamics, spread and suppression of epileptic seizures. To assist with the future focussing of this aspect of their research, the BRI asked the MISG 2010 participants to examine how the available EEG and fMRI data and current knowledge about epilepsy should be analysed and interpreted to yield an enhanced understanding about brain activity occurring before, at commencement of, during, and after a seizure. Though the deliberations of the study group were wide ranging in terms of the related matters considered and discussed, considerable progress was

http://anziamj.austms.org.au/ojs/index.php/ANZIAMJ/article/view/3638 gives this article, © Austral. Mathematical Soc. 2011. Published April 1, 2011. ISSN 1446-8735. (Print two pages per sheet of paper.) 

made with the following three aspects. (1) The science behind brain activity investigations depends crucially on the quality of the analysis and interpretation of, as well as the recovery of information from, EEG and fMRI measurements. A number of specific methodologies were discussed and formalised, including independent component analysis, principal component analysis, profile monitoring and change point analysis (hidden Markov modelling, time series analysis, discontinuity identification). (2) Even though EEG measurements accurately and very sensitively record the onset of an epileptic event or seizure, they are, from the perspective of understanding the internal initiation and localisation, of limited utility. They only record neuronal activity in the cortical (surface layer) neurons of the brain, which is a direct reflection of the type of electrical activity they have been designed to record. Because fMRI records, through the monitoring of blood flow activity, the location of localised brain activity within the brain, the possibility of combining fMRI measurements with EEG, as a joint inversion activity, was discussed and examined in detail. (3) A major goal for the BRI is to improve understanding about "when" (at what time) an epileptic seizure actually commenced before it is identified on an EEG recording, "where" the source of this initiation is located in the brain, and "what" is the initiator. Because of the general agreement in the literature that, in one way or another, epileptic events and seizures represent abnormal synchronisations of localised and/or global brain activity the modelling of synchronisations was examined in some detail.

# Contents

**1 Study group participation** **M39**

**2 Introduction** **M40**

**3 Background** **M46**

3.1 Epilepsy . . . . . M46

3.2 Electroencephalography (EEG) . . . . . M47

3.3 Functional magnetic resonance imaging . . . . . M50

**4 Predicting, detecting and/or monitoring seizure events M53**
4.1 Seizure prediction . . . . . M53
4.2 Change point monitoring and time series analysis . . . . . M54
4.2.1 Hidden Markov modelling . . . . . M54
4.2.2 Sudden change analysis . . . . . M55
4.2.3 Profile monitoring . . . . . M55
4.2.4 Sparse solution methodologies—independent component analysis . . . . . M56
4.2.5 Ordinary differential equation dynamical system modelling . . . . . M56
4.3 Modelling brain activity and epilepsy as synchronisation processes . . . . . M57

**5 Conclusions and future research M58**

**A Imbers: Epilepsy and seizure prediction M61**
A.1 Epilepsy and EEG . . . . . M63
A.2 Seizure prediction . . . . . M64
A.2.1 Analytical methods . . . . . M64
A.2.2 Methods . . . . . M65
A.3 Epilepsy models . . . . . M67
A.3.1 Macroscopic models . . . . . M69
A.3.2 Biophysical network models . . . . . M70
A.4 Summary . . . . . M71

**B Boland & Ward: Hidden Markov models and change point estimation M73**
B.1 Hidden Markov models . . . . . M73
B.2 Theory of hidden Markov models . . . . . M75
B.2.1 Changing the measure . . . . . M76
B.2.2 Updating estimates as new observations arrive . . . M77
B.3 Change point estimation . . . . . M79

B.3.1 Exponentially smoothed forecast variance . . . . . M80
B.3.2 Sample autocorrelation function . . . . . M80
B.4 Conclusion . . . . . M81

**C Bhavnagri: Analyzing for sudden changes or discontinuities M81**

**D Abdollahian et al.: Profile monitoring for brain activities M87**
D.1 Methodology . . . . . M89
D.2 The EWMA/R control charts . . . . . M91
D.3 Properties of EWMA . . . . . M93
D.4 Improving the forecasting ability of the EWMA chart . . . . M93
D.5 Conclusion . . . . . M94

**E Olenko: Independent component analysis for functional MRI M94**
E.1 The essence of ICA . . . . . M95
E.2 Simultaneous EEG and fMRI . . . . . M97

**F Anderssen: Synchronisation and the Kuramoto model M98**
F.1 The phenomenon of synchronisation . . . . . M99
F.2 The Kuramoto model . . . . . M100
F.3 The Kuramoto model and epilepsy . . . . . M101

**References M103**

# 1 Study group participation

Since this is the report of a MISG activity, many people contributed in various ways to its preparation. The authors of the report have been ably assisted by various colleagues, especially the ones who assisted with the preparation of the appendices: Jara Imbers (University of Oxford), John Boland and

Kathryn Ward (University of South Australia), Burzin Bhavnagri (Swinburne University of Technology), Mali Abdollahian, S. Zahra Hosseinifard, Nahid Jafariasbagh (RMIT University), Andriy Olenko (LaTrobe University) and Musa Mammadov (Ballarat University). Further details about the participants is contained in the Acknowledgements and the appendices.

# 2 Introduction

Even though brain function is an extraordinarily complex dynamic signalling and switching process, it is also a highly organised, robust and error correcting activity. This is reflected in numerous ways, such as the learning of languages by children, the skills of professional athletes, and the recall of highly complex matters.

This robustness not only ensures the successful and consistent functioning of the brain under normal and challenging circumstances, but is also the reason why, without fully understanding the finer details, consistent patterns in brain functioning are identified from appropriate indirect measurements, such as EEG and fMRI [1, 2] and subsequently and successfully utilised.

Historically, EEG proved quite successful in categorising the various forms of epilepsy. Its strength was that it recorded activity in the cortex and established that when abnormal activity occurred in a given patient, the abnormal activity was always localised to essentially the same place in the cortex and displayed stereotypical waveforms. The discovery that such information was directly recoverable from the EEG measurements highlighted the importance and utility of the EEG technology. This thereby established EEG as the basis for the syndromic classification of epilepsy into appropriate equivalence classes and as a key clinical tool in the diagnosis of epilepsy [3].

The weakness of EEG technology relates to the fact that it records the electromagnetic activity of the neurons within the brain because

- synchronous activity in about $10\,\mathrm{cm}^2$ of the cortex is required before it will be detected by the EEG [4], and
- high levels of electromagnetic activity near the surface of the brain mask out similar and even higher levels of activity deeper within the brain.

Mathematically, this weakness is reflected in the strongly improperly posed recovery of information about the location of electromagnetic sources within an object from surface measurements, which is the generic framework within which the analysis and interpretation of EEG measurements belongs. Consequently, identifying the sources within the brain which give rise to an observed EEG pattern reduces to solving a strongly ill posed inverse problem. In particular, the resolution of the location of a source decreases rapidly with depth. Electroencephalography (EEG) technology has the advantage that, as is visible in Figure 1, it accurately identifies the time of onset of synchronous cortical activity during an epileptic event or seizure. This is the reason behind the success, already mentioned, of EEG in the categorisation of different types of epilepsy.

However, as useful as it is from a clinical perspective, such categorisation has limited utility in enhancing understanding about the time and location of the internal initiation within the brain or the reason for the initiation.

With the development of fMRI technology [5], the possibility of combining fMRI measurements with EEG has become a key focus for research in the study of epilepsy.

The advantage of fMRI measurements is that they are used to identify the regions of blood flow and metabolic activity within the brain (Figure 2). For brain activity research, such reconstructions are fundamental for advancing the associated science, since it is known that brain activity associated with performing a specific task is associated with changes in blood flow and metabolism. The weakness of fMRI measurements is that their temporal resolution is poor.

This leads to the possibility, as a joint inversion activity [7], of matching

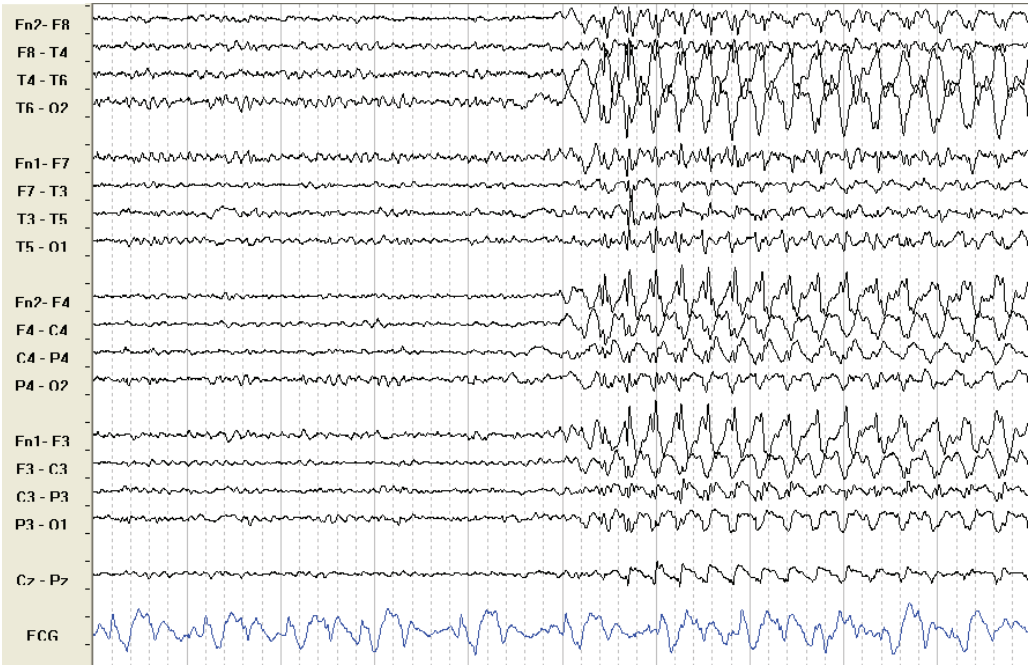


FIGURE 1: Electroencephalography (EEG) data showing onset of an epileptic event.

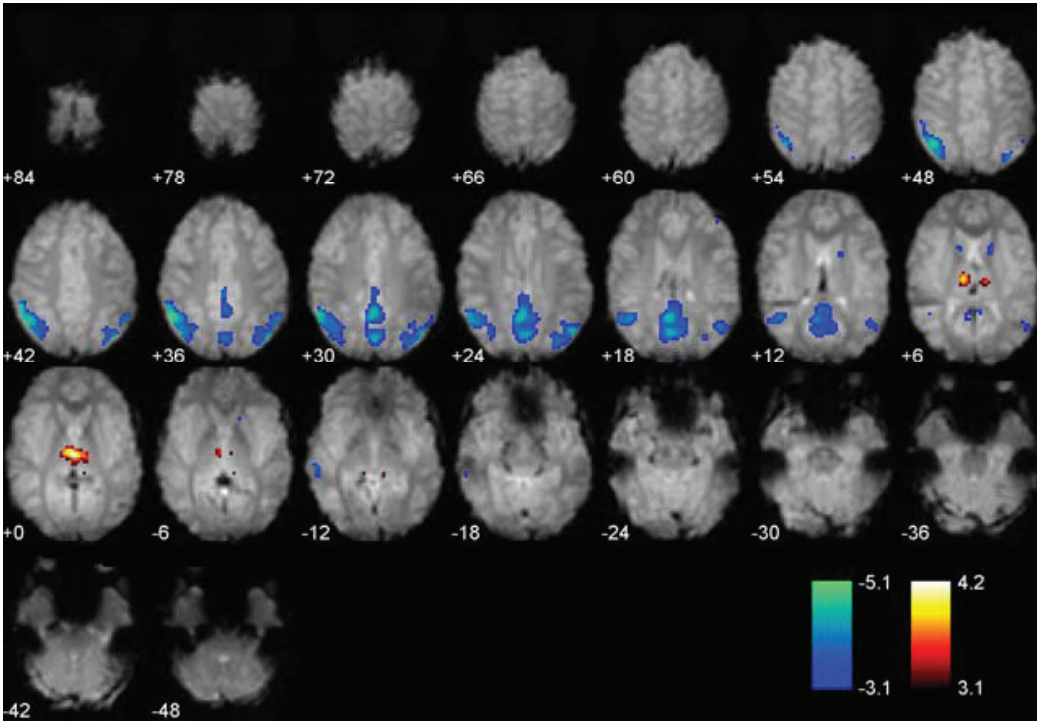


FIGURE 2: Functional Magnetic Resonance Imaging (fMRI) data showing localisation of BOLD signal changes [6].

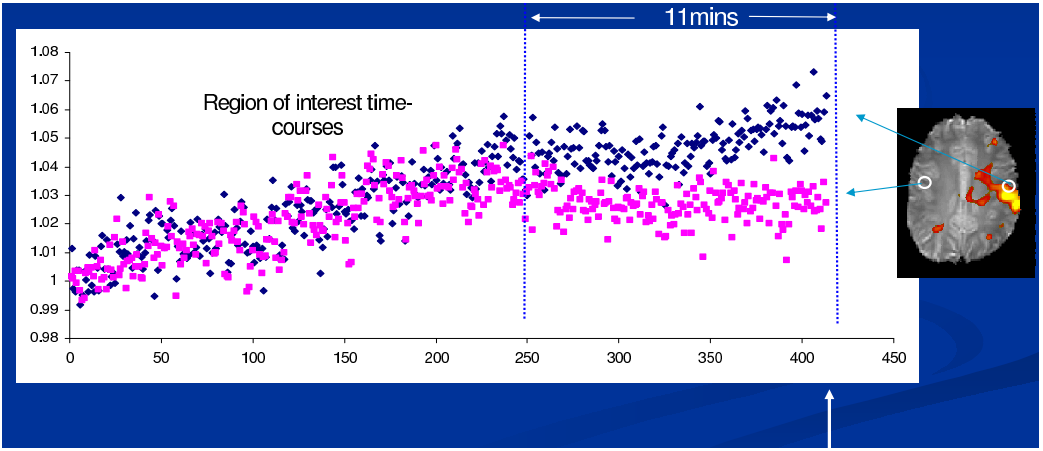


FIGURE 3: Functional Magnetic Resonance Imaging (fMRI) data showing localisation of blood flow and metabolic changes.

the advantages of EEG and fMRI measurements against their disadvantages. Section 2 explains that this type of joint inversion is already a key methodology currently being utilised to extend the utility of EEG measurements by using the EEG identification of the times that something interesting has occurred to look at the fMRI reconstructions to identify the locations where there was a high blood oxygenation dependant (BOLD) signal. Furthermore, recent studies have highlighted that fMRI may detect areas of brain activation that preceeds the onset of synchronous epileptiform activity as detected on the EEG. Figure 3 shows the changes in the variance and magnitude of the fMRI signal prior to a seizure [8, 9, 10, 11].

From the perspective of this joint inversion activity, the study group members were asked to examine the following questions:

- To what extent can the analysis of EEG and fMRI data be utilised jointly to assist with the identification of brain activity epilepsy precursors that precede the sudden change in EEG activity associated with an actual epileptic seizure? Here, the motivation was the need to explore how

information about the internal blood flow in the brain, as seen indirectly in fMRI data, contained precursor information not contained in EEG data which limits brain activity to the cortex.

- How can algorithmic protocols, developed in other contexts, be adapted to the monitoring of brain activity in patients with a known history of epilepsy? Here, the motivation was the exploration of possible monitoring protocols that could not only be used to recover new information about brain activity before, at the commencement of, during, and after an epileptic seizure but also be the basis for improving current clinical practice.

In the subsequent discussion of these and related questions, the following topics were examined in some detail:

1. The practical analysis and interpretation, as well as the recovery of information from, EEG and fMRI data (Section 3).
2. The practical joint utilisation of EEG and fMRI data for the identification of the time and location of the initiation of an epileptic event or seizure.
3. The prediction, detection and monitoring of seizures using various change point methodologies, such as hidden Markov chain and discontinuity identification methodologies, profile monitoring and independent component analysis (Section 4).
4. An analysis of the modelling of synchronisation from the perspective that the actual initiation of an epileptic event or seizure is a type of synchronisation of neuronal activity that gets out of control. The relevance, appropriateness and possible utilisation of the Kuramoto model of synchronisation was examined (Section 4).

# 3 Background

This section gives basic background necessary to clarify the industrial/medical framework within the current problem.

## 3.1 Epilepsy

Epilepsy is a family of disorders of the central nervous system characterised by abnormal brain activity and a predisposition to seizures (paroxysmal events). Epilepsy may arise secondary to some defined pathological process that affects the brain, or may arise in a brain that has no known abnormality. The International League Against Epilepsy (ILAE) proposed the formal definition of epilepsy as [12]

> a disorder of the brain characterised by an enduring propensity to generate epileptic seizures, and by the neurobiologic, cognitive, psychological, and social consequences of this condition.

In practice, this usually means two unprovoked seizures.

Seizures are paroxysmal events associated with changes to the patient's physical and/or cognitive state. Seizures are the clinical manifestation of excessive neuronal activity, which can arise abruptly and without apparent warning. Additionally, epileptiform discharges of short duration can occur in the interictal period (between seizures) without clinically detectable signs or symptoms—these are called interictal epileptiform discharges (IEDs). One of the fundamental goals of epilepsy research is to understand how epileptiform discharges are generated and what causes the brain to transition from its normal state of controlled signalling and synchronisation between neurons.

The ILAE defines a seizure as "a transient occurrence of signs and/or symptoms due to abnormal or synchronous neuronal activity in the brain" [12]. These signs and symptoms can vary greatly depending upon where in the brain the abnormal activity is located, and include such features as loss of consciousness,

convulsions and motor automatisms. Seizure types are broadly divided into two major classes: focal seizures, that occur within a focal region of one cerebral hemisphere; and generalised seizures, that have more than minimal involvement of both cerebral hemispheres. Within these main classes there are many subclasses depending upon the apparent region of onset of the abnormal brain activity and the symptoms of the seizure. This diversity of seizure manifestations reflects a variety of underlying mechanisms at the neuronal, cellular, and molecular levels.

Most often, these discharges occur briefly and in restricted regions of the brain. However, at times the discharges do not remain isolated in time or space, but spread, both locally and via synaptic pathways, to involve large areas of the cortex. The timing, location and extent of this spread leads to the variety of recognisable clinical symptoms of seizures.

It is not currently well understood why epileptiform discharges occur at particular points in time, or what causes the transition from the interictal state, where discharges are restricted in time and space, into the ictal state where there is sustained activity that spreads to wider cortical regions. It is not known what processes and interactions are required to create an environment where this hypersynchronous activity can take hold.

## 3.2 Electroencephalography (EEG)

The electroencephalogram (EEG) is a recording of electric potential changes associated with brain activity detected at the scalp. The scalp recorded EEG was first demonstrated as a measure of underlying human brain function by Hans Berger almost 80 years ago [13]. The source of the EEG is neuronal signalling, which results in the flow of ions into and out of the extracellular space, for example, the inward flow of $Na^+$ or $Ca^{2+}$ ions at an excitatory synapse. This ionic current flow is associated with a changing electric field within the extracellular space. When a sufficiently large population of neurons acts in concert, the changing electric fields can be detected by EEG electrodes

located on the scalp.

The electric fields associated with synaptic activity in a single neuron are very weak and rapidly decay with distance. Even when an electrode is placed very close to the cell, the measured extracellular potential may only be in the order of microvolts. This means that an electrode placed at a distant site will generally be unable to measure the activity of a single neuron.

The extra-cellular potentials that are detected with EEGs represent the summed activity of many neurons that lie in the cortex beneath the scalp electrodes. If the neurons are acting asynchronously, in other words if there is no correlation in the activity between the different neurons, the electric fields will tend to destructively interfere with each other and no net electric field will be detectable at the scalp. However, when the neurons act in synchrony the electric fields associated with each individual neuron will add constructively and produce a relatively large electric field that is detectable at the scalp.

The EEG is effectively 'blind' to much of the brain's activity, be that because the activity is asynchronous, is located in a relatively small region, is not in the cortex, or it does not involve parallel aligned neurons. It has been estimated that cortical sources any smaller than $6\,cm^2$ cannot be detected by EEG at the scalp and that, for reliable detection, at least $10\,cm^2$ of synchronously active cortex is probably required [4]. Whilst this undoubtedly is a limitation of EEG, it does also provide certain advantages. For example, synchronisation plays an important and necessary role in coordinating neurons in order to perform complex tasks, so the EEG's sensitivity to this kind of activity may actually help focus attention upon the most interesting aspects of brain function. Any interpretation of underlying neuronal activity based upon the EEG must be formed in recognition of the fact that it does only provide a partial picture of the brain's activity.

Often the aim of an EEG study is to spatially localise the underlying source(s) of scalp detected voltage changes that are associated with an event of interest. To provide this localisation, the EEG may be analysed either visually or by more sophisticated source modelling techniques. Visual analyses use a

comparison between the EEG recordings from different electrode positions and will generally provide spatial localisation to a cortical area under one or more of the electrodes, whereas source modelling techniques aim to provide more detailed spatio temporal descriptions of the sources.

Source modelling analyses attempt to estimate the location of the underlying source(s) that could generate the observed voltage distribution at the scalp. However, source modelling results do not represent images of actual physiological change. They are based upon mathematical modelling and, in particular, involve the solution to an ill-posed inverse problem which requires introducing constraints and prior expectations into the modelling [14]. This means, for example, that a widespread cortical source region may be erroneously modelled using a dipole located deeper within the brain below the scalp [15]. This highlights that the accuracy of source localisations are highly dependent upon the choice of the source model. Consequently, when using EEG source modelling, the resultant spatial localisation should be interpreted as an approximation based upon a pre-defined model rather than a reflection of the actual underlying source.

Beyond the patient's clinical history, the EEG is the most common diagnostic test for epilepsy and is generally obtained for each patient. The hypersynchronous neuronal activity associated with epileptiform discharges produce recognisable EEG patterns that can assist in differentiating and classifying the type of seizure and syndrome, and provide localising information. In particular, combining long term EEG recordings with video monitoring provides detailed data on seizure symptoms and the epileptic relationship to the onset and evolution of the electrographic activity. Analysis of EEG recordings in epilepsy studies is mainly based upon visual qualitative assessment and relies upon the experience and expertise of the electroencephalographer. Quantitative EEG analyses, such as dipole localisation analyses, better characterise and localise epileptiform activity.

## 3.3 Functional magnetic resonance imaging

Functional magnetic resonance imaging (fMRI) is a technique for measuring metabolic and blood flow changes in the brain. This provides a surrogate marker for neuronal activity, because synaptic activity causes localised increases in energy usage and resultant localised increases in aerobic metabolism and blood flow. Functional MRI, therefore, provides information regarding the spatial localisation of brain function, and thereby compliments the data coming from simultaneous EEG studies.

Functional MRI relies upon the magnetic properties of haemoglobin, a protein in red blood cells used to transport oxygen, to provide information about local blood flow and metabolism changes in the brain. Within an externally applied magnetic field, there is a magnetisation difference between oxygenated haemoglobin (oxyhaemoglobin) and de-oxygenated haemoglobin (deoxyhaemoglobin). This magnetisation difference is used by fMRI to detect changes in the relative concentration of these two different states of haemoglobin within the blood. Functional MRI images are said to have a blood oxygenation level dependent (BOLD) image contrast [16]. Sequential acquisition of BOLD weighted images provide a time course of the changes in this physiological parameter and are used as a measure of brain function.

The predominant feature of a time course BOLD signal evoked by a task or stimulus is an increase in the signal intensity above baseline [17]. This BOLD signal increase is delayed and dispersed in time relative to the application of the stimulus [5, 18, 19, 20]. Although the peak BOLD signal change is larger than the instrumental noise in modern MRI scanners [2], there are other sources of noise in the BOLD signal time course that induce further signal changes on top of those evoked by the stimulus. This includes head motion, cardiac pulsation and respiration [21, 22, 23]. Furthermore, spontaneous fluctuations in the BOLD signal baseline due to ongoing neuronal activity contribute significant low frequency noise in the context of a task related fMRI experiment, although there has been recent interest in the potential for such signal fluctuations to reveal major functional networks of the brain [23]. The

effects of some noise are somewhat mitigated by approaches such as spatial realignment of the images to compensate for subject movement between each acquisition [24] and the filtering the time course BOLD signal to remove effects due to motion, cardiac pulsation and respiration [25, 26]. However, such post-acquisition corrections cannot remove all the noise and fMRI experiments generally require many trials to reliably detect the BOLD signal changes associated with a given stimulus.

The relationship between the stimulus and evoked BOLD signal time course is well approximated by a linear transform model [22]. However, there are some situations where non-linearities may be observed. For example, Friston et al. [27] demonstrated that, for stimulus separations of one second the BOLD signal changes may show non-linearities, which means that the amplitude and duration of BOLD signal changes evoked by a stimulus may be affected by prior stimulus during the previous second. However, in practice these non-linearities are generally avoided in most fMRI experiments and the linear transform model provides a good approximation.

Under the assumption of a linear transformation, the mapping between the experimental stimulus and the expected BOLD time course can be performed using a linear convolution operation [22]. This convolution produces a prediction of the experimentally evoked time course of the BOLD signal changes, which correlated to the observed signal changes at each voxel [22, 21].

Functional MRI can provide very high resolution images of brain function. Rapid imaging techniques give an in-plane spatial resolution of a few millimeters (in the brain). Higher spatial resolution images with sub-millimeter in-plane resolution can be acquired using multi-shot image acquisition sequences, if a lower temporal resolution is acceptable [20]. However, the spatial resolution with which an fMRI image is acquired at does not determine the intrinsic sensitivity of the technique to resolve the location of brain activity. The true resolution of fMRI is better described by how closely the detected BOLD signal changes spatially co-localise to the underlying neuronal activity. In particular, the BOLD contrast originates from magnetic field gradients sur-

rounding blood vessels containing deoxyhaemoglobin. This effect is detected over a larger spatial area than the underlying active neuronal population and is also dependent upon the orientation of the blood vessels relative to the magnetic field [16]. Estimates of the maximum spatial resolution obtainable with BOLD contrast imaging suggest that it may be a few millimeters, irrespective of voxel size [28, 29]. This fine spatial resolution is far greater than is available with EEG source modelling. Importantly, it does not rely upon the many assumptions needed by EEG source modelling techniques.

The effective temporal resolution of fMRI is dependent upon two factors: the speed of the image acquisition itself; and the haemodynamic response function. The fMRI image acquisition places a fundamental limit upon how rapidly the BOLD signal can be acquired. Blood oxygen level dependence (BOLD) contrast imaging relies upon differences in the $T_2^*$ relaxation of parenchymal tissue due to the blood oxygenation level in nearby capillaries and venules. Therefore the echo time of a BOLD weighted image sequence must be chosen to provide a good contrast between the oxygenated and de-oxygenated states, which was shown to be optimal when $TE \approx T_2^*$ [30]. In a MRI scanner, this means that the optimal BOLD contrast is provided by images acquired with an echo time of about 50, which limits the speed of imaging. Furthermore, this is a per-slice limit, so, if whole brain imaging is required, the total acquisition time is generally at least two seconds. However, regardless of how quickly the fMRI images are acquired, the haemodynamic response function places a limit on how closely the BOLD signal can resolve the underlying brain activity. The hemodynamic response function, as measured by the fMRI, effectively smooths the underlying brain activity, which makes it difficult to resolve the timing to less than a second. This imposes a more dominant and fundamental limit on fMRI. It means that BOLD fMRI cannot provide a measurement of brain activity with a temporal resolution of much less than one second, even if only rapid single-slice imaging is performed.

# 4 Predicting, detecting and/or monitoring seizure events

As mentioned in the Introduction and illustrated in Figure 3, there is growing evidence that a change in fMRI activity between different key regions in the brain are a precursor to a seizure, at least for some types of epilepsy. It was this observation which initiated an examination of methodologies for detecting change and how they might be adapted for predicting and detecting the onset of a seizure. A subset of such procedures are also ways for monitoring a patient before, during, and after a seizure.

Such procedures are examples of practical expedient of directly using the dynamics and structure in the indirect measurements to solve the underlying inverse problem. Such a strategy avoids the need for involved computational inversion techniques. To be applicable, inversion techniques must exploit specific information about the phenomenon under investigation which directly relate the measured data to the question that must be resolved. In the current situation, the specific information to be exploited is the existence of epileptic seizure precursors such as the fMRI example of Figure 3.

## 4.1 Seizure prediction

Seizure prediction, because it is so fundamental to the successful clinical treatment of the ailment, is the major focus of epileptic research from clinical, practical and theoretical perspectives. This is reflected in the large number of publications addressing either directly or indirectly. Appendix A comprehensively surveys the literature from a seizure perspective. In particular, after a general introduction about the brain, the appendix addresses the following issues: epilepsy and EEG; analytic and non-linear methodologies for seizure prediction; models of epilepsy including macroscopic and biophysical network formalisms.

## 4.2 Change point monitoring and time series analysis

In change point monitoring, the goal is the formulation of methodologies which sensitively detect the type of change which defines the precursor of the event to be predicted. Because of the generic nature of precursor detection there are a variety of methodologies that have been adapted to performing some form of *'change point monitoring'*. Addressed in some detail during the study group deliberations were *'hidden Markov chain modelling'*, *'sudden change analysis'*, *'profile monitoring'*, *'dynamical systems modelling'* and *'independent component analysis'*.

### 4.2.1 Hidden Markov modelling

From classical time series analysis, there are two principal questions addressed when analysing EEG series. One is the determination of the number of possible states of the system and their respective characteristics. One can suppose a priori that there are two states, seizure and non-seizure. Such an assumption may well eliminate the identification of potentially important states; for instance, a pre-seizure state. If such a state exists and is not identified, knowledge of possibly the most important state, that of a pre-cursor to a seizure event, is lost. For this reason, the use of the hidden Markov model (HMM) is proposed to help determine the number and characteristics of the states being examined through the EEG. A Markov chain is a probabilistic process over a finite set $\{s_1, \ldots, s_N\}$ the elements of which are known as "states". Interest is usually in the probability that a future state $X_{k+1}$ is $s_i$, given the current state, $X_k$, $\Pr(X_{k+1} = s_i \mid X_k)$. A hidden Markov model (HMM) is a Markov model in which some of the states are unobservable [31, 32]. We can see only the effect that the hidden states have on the other variables. Each state within the model has a probability distribution over the possible output observations. Thus the sequence of observations generated from the HMM gives information about the sequence of the states (hidden and visible). Appendix B contains quite detailed explanation.

The second question involves the determination of the timing of a change of state. Two possible methods are described below for identifying change points in the processes. The first method identifies a change in the variance of the EEG time series. Since variance is unobservable, we need an estimation method for the variance at time $t$. The second method is the exponentially smoothed forecast variance described in detail in Appendix B. In essence, a smoothed version of the conditional variance is formulated and used to determine when there are significant changes in the time series data.

### 4.2.2 Sudden change analysis

In the modern theory of image analysis [33, 34, 35], very sophisticated methodologies have been formulated and implemented for discontinuity identification and sudden change analysis. Appendix C discusses how the techniques developed for image analysis might be adapted to epileptic seizure identification.

### 4.2.3 Profile monitoring

In many quality control applications, the performance of a process or a product is characterised and summarised by a relation (profile) between a response variable and one or more explanatory variables. Such profiles are modelled using linear or nonlinear regression models. Profile monitoring uses control charts to monitor the quality of a process/product profile and detect the size and type of shifts in the shape of the profile which is often represented by the parameters of the regression model. Functional magnetic resonance imaging (fMRI) data from a single 'run' consists of a time series of three dimensional images while the subject is performing a task or receiving a stimulus inside the scanner.

An extension is proposed of the application of profile monitoring as a possible strategy for monitoring the brain activities of epilepsy patients. The aim is to fit an appropriate model to brain activities based on one or more

independent explanatory variables. Exponentially weighted moving average (EWMA) control charts are then used to: monitor the coefficients resulting from a model fitted to profile data; predict the next value for the brain activity; monitor brain activities and observe which regions of the brain are activated by the task or stimulus; locate regions of the brain where the changes are significant (based on frequently of out of control signals); and to monitor the size and trend of the changes that lead to the onset of seizure.

Frequency of the out of control signals in each region of the brain could also aid the practitioners to decide which regions of the brain have out of control activities. It is hoped that this information will provide a prognosis tool for the medical practitioners to make informed decision on the forecasting/ prevention of and treatment of patients. The proposed profile monitoring scheme is capable of forecasting the response value for the next period based on the values of the present response and one or more explanatory variables. Appendix D discusses full details.

### 4.2.4 Sparse solution methodologies—independent component analysis

Independent component analysis (ICA) has been applied at the BRI on pre-ictal fMRI data with preliminary results suggesting it may be capable of separating components related to epileptiform activity [36]. Although independent component analysis (ICA) was only briefly discussed during the study groups' deliberations, it was viewed to be of sufficient importance to have some information about it included. Appendix E gives some detail.

### 4.2.5 Ordinary differential equation dynamical system modelling

BOLD fMRI activity is recovered as a discrete time series for each of the $n$ voxels of the brain:

$$X(t_i) = (x_1(t_i), \ldots, x_n(t_i)), \quad i = 1, \ldots, I\,. \tag{1}$$

As already indicated, there are various ways in which this time series encapsulation of whole brain activity can be modelled.

Another possibility is to view the time progression of the $\mathsf{X}(\mathsf{t}_i)$ as the realisation of a dynamical system. It is then natural to turn to the use of systems of ordinary differential equations, possibly involving time delays, to model the time progression in terms of parameters that reflect the nature of the assumed brain activity. One possibility would be to exploit the control systems methodology as proposed by Mackey and Glass [37]. Another approach would be to utilise such time series data to identify the parameters in a Kuramoto model, as described in Appendix F.

## 4.3 Modelling brain activity and epilepsy as synchronisation processes

As is clear from the above discussion, the bulk of the study group's deliberations focussed on understanding the nature of epilepsy, the sources of data, the interpretation of the data, the importance of change point analysis, and discussing methodologies for detecting, predicting and monitoring brain activity. However, some time was given to a discussion about how one should model brain activity mathematically from the perspective of epilepsy being some failure of the normal activity. The published literature indicated that brain activity can be viewed as a multi-level synchronisation process. Modelling of synchronisation has been extensively studied mathematically in the context of brain waves, sleep, fireflies, superconductivity, etc [38].

From the plots of EEG recordings of epileptic events/seizures, such as is shown in Figure 1, the rapid onset of the highly oscillatory phases can be viewed as occurring through some major synchronisation activity within the brain. There is strong agreement that this is representative of the brain activity occurring prior to, at and during a seizure [39]. However, in modelling such synchronisation, the appropriateness of the Kuramoto model [118] has not been explicitly examined. In the context of epilepsy, this model has been

indirectly mentioned as an example of the brain being a complex network which synchronises.

The role of Appendix F is an examination of the extent to which the Kuramoto model represents a basis for modelling the synchronisation associated with epilepsy, and also to determine the extent to which this model might provide insight about the nature of the synchronisation occurring.

# 5 Conclusions and future research

The Brain Research Institute (BRI), at Austin Hospital, uses various types of indirect measurements, including EEG and fMRI, to understand the initiation, dynamics, spread and suppression of epileptic seizures. In order to assist with the future focussing of this aspect of their research, the BRI asked the MISG 2010 participants to examine how the available EEG and fMRI data and current knowledge about epilepsy should be analysed and interpreted to yield an enhanced understanding about brain activity occurring before, at commencement of, during, and after a seizure.

As a result of the initial deliberations and subsequent discussions of the study group members, the following three matters were identified and became the focus for the contributions that could be made, in the time available, to give suggestive and potentially useful answers to the questions raised by the BRI, as outlined in the Introduction:

1. The formulation of methodologies for the prediction of the onset and subsequent monitoring of an epileptic seizure.
2. The joint utilisation of EEG and fMRI data in the investigation of item 1.
3. The modelling of epileptic seizures as a multiple synchronisation processes.

This report gives, in Section 3 and Appendix A, a detailed summary of

relevant aspects of current epilepsy assessment, management and research. The major focus of the report, which directly reflects the focus of much of the discussions of the study group, is the various suggestions for performing change point analysis. A summary of the various suggestions is given in Section 4 with the finer details contained in a series of appendices. Together, the material in Sections 3 and 4 and the associated appendices, represent the study groups contributions to items 1 and 2.

At a lower level of activity, the study group explored the possibility of using the Kuramoto model of synchronisation as a basis for the mathematical modelling of epileptic seizure initiation. This is reviewed in Section 4.3 and discussed in greater detail in Appendix F.

The above discussion highlights how the results, suggestions and conclusions given in this report yield a foundation for future research opportunities that the BRI can consider pursuing. With respect to all the matters discussed in this report, there are future research opportunities from both practical and theoretical perspectives. The various suggestions for change point monitoring fall into the practical category. Discontinuity identification, sparse signal recovery, ICA and synchronisation modelling represents interesting and challenging theoretical research opportunities.

In summary, the success of the study group's activities is reflected in the following achievements:

- Prediction, detection and monitoring abnormal brain activity or events using various change point modelling and time series analysis techniques. These techniques include methodologies for detecting change as a precursor to an epileptic seizure and procedures for patient monitoring before, during and after an epileptic event. Hidden Markov modelling, sudden change analysis, profile monitoring and independent component analysis were presented as part of this.
- Modelling of brain activity and epilepsy as a synchronisation process via the Kuramoto model.

From this work we concluded that it is important to provide quality analysis, interpretation and recovery of the information from EEG and fMRI measurements which will further develop the understanding of the science behind brain activity. Using both the EEG and fMRI data, as a joint inversion problem, provides the opportunity to explore spatial localisation of epileptic activity. These techniques give an opportunity to answer the 'when', 'where' and 'what' questions associated with epileptic seizures.

**Acknowledgements** The Moderators thank all the participants who contributed in various ways to the deliberations and discussion. They were David Abbott, Mali Abdollahian, Burzin Bhavnagri, John Boland, Philip Broadbridge, Sandra Clarke, Jara Imbers, Seyedeh Hosseinifard, Nahid Jaifariasbagh, Musa Mammadov, and Andriy Olenko. Thanks from all of us to John Shepherd and his RMIT colleagues for organizing such a stimulating and enjoyable MISG. In particular, special thanks go to the colleagues who prepared appendices:

**Appendix A** Jara Imbers; OCCAM, The Mathematical Institute, University of Oxford; Epilepsy and seizure prediction.

**Appendix B** John Boland and Kathryn Ward; Institute for Sustainable Systems & Technologies, School of Mathematics and Statistics, University of South Australia; Hidden Markov models and change point estimation.

**Appendix C** Burzin Bhavnagri; Centre for Molecular Simulation, Swinburne University of Technology; Analyzing EEG and fMRI data for sudden changes or discontinuities.

**Appendix D** Mali Abdollahian, S. Zahra Hosseinifard, Nahid Jafariasbagh; School of Mathematical and Geospatial Science, RMIT University, Melbourne, Victoria; Profile monitoring for brain activities using fMRI data to locate the onset of seizure.

**Appendix E** Andriy Olenko; Mathematics and Statistics, LaTrobe Univer-

sity, Bundoora, Victoria; Independent component analysis (ICS) for fMRI.

**Appendix F** Robert (Bob) S. Anderssen; CSIRO Mathematics, Informatics and Statistics; Synchronisation and the Kuramoto model.

# A Jara Imbers: Epilepsy and seizure prediction

The brain is among the most complex systems in nature. The brain contains about 15–20 billion neurons and each neuron is linked to another neuron by up to 10 000 synaptic connections. As a result, each millimeter of cerebral cortex contains approximately one billion synapses. The cerebral cortex is connected to various subcortical structures such as the thalamus and the basal ganglia. Information between these structures is sent and received via synapses [41]. Despite the rapid advancement of neuroscience, much about how the human brain works remains a mystery. Operations of individual neurons and synapses are understood in considerable detail, and it is known that the dynamical behavior of individual neurons are governed by integration, threshold and saturation phenomena. Much less is known about the way in which neurons cooperate. Given the highly interconnected neuronal network in the brain, it is not surprising that neuronal activity results in various synchronised activities, including epileptic seizures, which often appear as a transformation of otherwise normal brain rhythms. Methods of observation such as EEG recording and functional brain imaging reveal that brain operations are highly organised. However, more research needs to be done to be able to address the underlying processes that govern the brain.

The focus of this report is to investigate what is known about the dynamics of the brain prior to epileptic events. This is undertaken through analysis of the differences in the dynamical behavior of a patient brain compared to that of a control group.

We begin by giving the most commonly accepted definition of epilepsy and seizure given by Fisher et al. [12]: epilepsy describes a disorder of the brain characterised by an enduring predisposition to generate epileptic seizures. This definition requires the occurrence of at least one epileptic seizure. A seizure in turn is a transient of signs and/or symptoms due to abnormal excessive or synchronous neuronal activity in the brain [12]. Generalised onset seizures involve almost the entire brain, while focal onset seizures originate from a circumscribed region of the brain, called the epileptic focus, and remain restricted to this region [6]. Epileptic seizures may be accompanied by an impairment or loss of consciousness, sensory symptoms, or motor related phenomena.

The signs and symptoms previous to a seizure are numerous and seem to depend on the patient, which makes understanding epileptic events challenging for both the clinician and from an academic point of view. More than 50 million of individuals suffer from epilepsy worldwide (approximately 1% of the world's population) and in 25% of epilepsy patients seizures cannot be controlled by any available therapy. For these patients, the sudden and unforeseen way in which epileptic seizures strikes them can be disabling. Hence, a method capable of predicting the onset of a seizure would significantly improve the therapeutic possibilities and thereby the quality of life of patients.

During the last three decades most research focused on the development of EEG analysis techniques that aim to identify seizure precursors and combined these with fMRI or other imaging techniques. To date no definite information is available as to how, when or why a seizure occurs. Before we can propose new routes of investigation in the field of epilepsy prediction, we should revise the findings and contributions of an extensive scientific community working in this area.

## A.1 Epilepsy and EEG

When combined with fMRI, EEG analysis techniques offer an important way to identify seizure precursors. As an example, EEG allows the direct study of brain responses, which is crucial given that the clinical symptoms are too varied to be useful for prediction. Supporting clinical symptoms with independent results from the EEG analysis provides a very powerful tool for monitoring patients. EEG has often a close relationship with some physiological and pathological functions of the brain, and as a consequence, EEG has become a key component of the diagnosis of epilepsy.

The electrical activity recorded using EEG is generated by post-synaptic sum potentials of cortical neurons and results from a superposition of a large number of individual processes. The synaptic connections between neurons have an excitatory or inhibitory nature. The aggregation of these processes is recorded by the EEG. Hence, the duration of a seizure and changes in brain activity prior to an event can be observed by an EEG recording. Identification of the characteristic changes in EEG recordings preceding seizure onset is very important in seizure prediction.

Combining the high temporal resolution of EEG with the high spatial resolution of imaging technologies, like magnetic resonance, provides a unique opportunity to advance the understanding of epilepsy.

From a theoretical point of view, Lopes da Silva [42, 43] proposed two different scenarios about how a seizure could evolve. In the first scenario, a seizure can occur with a sudden and abrupt transition in brain activity dynamics, in which case it would not be preceded by detectable dynamical changes in the EEG. This scenario is thought to occur in cases of generalised epilepsy.

In the second scenario, the transition is a gradual change in brain activity dynamics, which is detectable. This scenario is more likely in focal epilepsies which assumes there exists a preictal state. It is easier to postulate the existence of an earlier transitional preictal state given that a seizure has already been with the EEG. However, a robust definition of such a state

and with it, its possibility to predict an impeding seizure, is a much harder mathematical problem. For the time being, one can assume the existence of a preictal state based on recent investigations that have found physiological and clinical support for the idea that certain types of seizures are predictable, [44, 45, 46, 47, 48, 49]. Functional MRI based evidence of transitional states preceding seizures [8] and interictal spikes [50] can also lend support to this hypothesis. Section A.3 presents theoretical models to aid the understanding of a preictal and ictal state, the remainder of this report assumes their existence based on experimental evidence.

## A.2 Seizure prediction

Research on seizure prediction has a long history. There are numerous reviews that contain detailed information that refer to the different methodologies [51, 53, e.g.]. Generally, these methodologies originated in different fields of study and were eventually applied to seizure prediction. Research into prediction of rare and extreme events has risen in many scientific areas, such as physics, mathematics, geophysics, meteorology and economics.

### A.2.1 Analytical methods

Initially, EEG recordings were analyzed using linear methods such as pattern recognition, analytic procedures of specral data and autoregressive modelling of the EEG recordings. In these models, mathematical techniques were used to detect the preictal phase from EEG recordings, where the existence of a preictal state was assumed based on experimental evidence as mentioned above. It was reported that seizures could be predicted several seconds, minutes or hours before occurrence, depending on the technique. For instance, autoregressive modelling [54, 55] found pre-ictal changes in the modeled parameters up to six seconds before seizure onset.

Pattern recognition had also been used to analyse spiking rates in epileptic

patients. These models have been shown to possess no predictive value. Similarly the predictive value of spike occurrence rates from EEG recordings via several linear methods also showed no systematic and robust changes in spike rates occurring prior to a seizure [56, 57, 58].

### A.2.2 Methods

Further development on seizure prediction led to combining linear methods with new models based on theoretical aspects of nonlinear dynamics [60]. These methods have been easily justified by their ability to enhance the complex dynamics of the brain; however, they did not rule out the possibility of linearity. Linear techniques had proved a valuable contribution to the field through improvement in the general understanding of the physiological and pathological conditions in the brain. However, linear models only provide limited information about the dynamics of EEG.

It is argued that nonlinearity is introduced in brain dynamics even at the cellular level, given that the dynamical behavior of individual neurons is governed by integration, threshold and saturation phenomena. Thus, in order to charaterised the complex and irregular dynamics of the brain it becomes necessary to use nonlinear dynamical systems.

In this context, the transition from no seizure to a seizure has been hypothesised to be caused by an increasing spatial and temporal nonlinear summation of the activity of discharging neurons [61]. Thus, EEG recordings were analyzed by looking at their Lyapunov exponents, dimensions, entropies or correlation densities, which are widely used as measures of nonlinear dynamics [62, 63, 64]. The main disadvantage of these measurements comes from the difficulty in the interpretation in terms of their physiologic correlation. Various studies looked for neurophysiologic features from EEG recordings associated with epilepsy, such as burst of complex epiletiform activity, slowing, chirps and in signal frequency.

A common property of the linear and nonlinear methods previously mentioned

was that they focused on univariate measurements and related only to a single recording site. Because of this, the measurements do not reflect the interactions between different regions of the brain. This is an important limiting feature given that a seizure is commonly accepted to be closely associated with changes in neuronal synchronisation. To counteract this research was then focused on analyzing EEG recordings by looking at bivariate or even multivariate measurements based on synchronisation and nonlinear dynamics [65, e.g.]. The development of these techniques allows for the assessment of synchronised activity from multiple sites and include nonlinear interdependence, measures of phase synchronisation and cross-correlation.

Results clearly indicated that seizures are not random events and are related to ongoing dynamic processes that may begin minutes to days before an epileptic event. This is further complicated by different techniques measuring different times over which seizures occur. None of the techniques discussed fully captures the full dynamics of the brain activity because each of measurement only depicts one aspect of the origin of a seizure. Furthermore, patterns of brain activity vary from patient to patient and it appears that different approaches may be required to predict seizures with clinical usefulness and accuracy in different individuals or in different epilepsy syndromes.

At present, EEG analysis techniques are only sufficient for general clinical application and many issues still need to be overcome in terms of analysis. This was shown by the International Seizure Prediction Group (ISPG) formed in 2000 to address these issues. Their purpose is to carry out rigorous methodological designs in seizure prediction and show that many of the methods described above did not perform better than a random predictor. On the other hand, a statistically based evaluation of the capabilities of a number of linear, nonlinear, univariate and multivariate measures to distinguish the preictal from the interictal state has provided evidence of significant differences in EEG characteristics between the two. Bivariate and multivariate measures were generally more effective for prediction [52]. Thus, in order to evaluate whether seizures are predictable by these methods, further studies need to rely on sound and strict methodology and include rigorous statistical validation.

This needs to be undertaken with the collection of experimental data across different sources to ensure that EEG recordings and other sources of data are complete sets and provide sufficient variability of brain activity.

## A.3 Epilepsy models

Section A.2 reviewed an extensive literature on seizure prediction. A common feature of methodologies is that they analyse the output of EEG recordings without investigating the underlying mechanisms that govern brain dynamics both on a normal brain and on an epileptic brain. Results across various individuals are then very difficult to compare and combine together which makes it hard to draw meaningful conclusions. Of course, the motivation in exploring these techniques is that the brain is a very complex system far from being fully understood and at times these methods are the best tools for analysis.

In order to improve knowledge of brain activity and to support previous research, robust mathematical models have been formulated. Theoretical and computational models have advanced the understanding of brain dynamics by providing a framework in which to compare the experimentally observed EEG patterns. Lopes da Silva et al. [42] redefined epilepsy as a dynamical disease of the brain. Most of the methodologies described previously in this appendix assume the existence of a type of preictal state. The ideas of Lopes da Silva et al. serve as the foundation of current time series analysis and provides the most promising future research in this area.

Lopes da Silva et al. [42, 43] emphasised the need to understand epilepsy based on both neurophysiology and nonlinear systems. Thus, one can describe the brain as a complex and highly dimensional dynamical system with multi(bi) stable states. Hence, the brain can display bifurcations for such states. For simplicity we assume that two states are possible: an interictal one characterised by a normal steady state of ongoing activity; and another one charaterised by the sudden occurrence of synchronous oscillations—a seizure.

Using the terminology of dynamical systems we say that this bistable system has two attractors and the transition between the normal ongoing activity and the seizure activity can occur according to three models. The first model applies to a type of epileptic brain in which the distance between the attractors of the normal steady state and seizure state are very close in comparison with a normal brain. Thus, small random fluctuations of some variables in the brain trigger a bifurcation which is typical of a generalised seizure in the brain. This is not predictable. The second and third model correspond to another type of epileptic brain which typically occur in patients who suffer from localised seizures. In these models the distance between the two different attractors is, in general, large so that random fluctuations are not enough for a bifurcation to occur. However, these brains have abnormal features that mathematically are characterised by parameters that are vulnerable to the influence of endogenous or exogenous factors. These parameters might vary gradually with time in such a way that the distance between the two attractors gets shorter and this can lead to a transition to a seizure.

The three models form a theoretical picture which presents a framework for understanding changes in the EEG recordings. According to these models, the changes of the system's dynamics preceding a seizure may be detectable in the EEG recordings. Hence, the route to the seizure may be predictable as presented in the second and third model. Alternatively the changes may be unobservable using measurements of the dynamical state forming the basis for the first model. Electroencephalography (EEG) recordings are consistent with the first model of epilepsy and methods inspired by nonlinear dynamics are in agreement. Thus, one route in which to continue research is towards the understanding of the different dynamical states of neuronal networks based on a combination of neurophysiology together with theoretical and computational models.

It is in this context that numerous models for brain activity and epilepsy have been developed. In general terms we could divide some of these models into two categories: macroscopic and biophysical network models. These two catagories provide the theoretical basis for the computational models that aim

to understand the brain and epilepsy as a dynamical disease. Any model of brain activity tries to capture the synchronised neural activity, as it seems to be prevalent in many areas of the brain. Synchrony can occur on the spike to spike level or on the bursting level, and is usually associated with oscillatory activity. Oscillations may be generated by intrinsic properties of cells or may arise through excitatory and inhibitory synaptic interactions within a local population of cells.

### A.3.1 Macroscopic models

In macroscopic models the brain is thought to be a high dimensional nonlinear dynamical system. One can assume that its dynamics can be charaterised by a much lower dimensional space as suggested by EEG recordings. The macroscopic models are the mean field models and they are typically an extension of the pioneering Wilson Cowan model [66]. Wilson and Cowan introduced this rate based population model of cortical tissue based on the idea that the identity of the presynaptic neuron is not important. Instead, they focused on the distribution of the level of activity. Thus, the model equations do not include biophysical details. This leads to a statistical description of brain activity in which the population of active neurons is chosen as a model variable. Often the justification for this statistical approach is given in terms of the spatial clustering of neurons with similar response properties in the cortex. Wilson and Cowen's model is the first generation of a series of more sophisticated models that have been developed since. Results show that these models have been able to simulate various experimentally observed EEG patterns. Overall, these models aid the understanding of brain activity and epilepsy by providing a way to look into transitions from interictal and ictal states. The models are particularly useful for the analysis of the EEG recordings from epileptic patients since the macroelectrodes used for EEG recordings represent the average local field potential arising from neuronal populations similar to those in the described statistical models.

The Kuromoto model provides a basis for modelling the neuronal synchronous

phenomenon that arises in epilepsy. Appendix F describes this model. Note that this model can be thought of as a macroscopic model and thus it gives the evolution of a synchronised population of neurons which could be collected on one electrode of the EEG. Alternatively this model can emulate the dynamics of a single neuron coupled to the rest of the network. In order to see the usefulness of this model in describing brain activity, one can think of the following basic process: the axon of a neuron is connected via synapses to the dendrites of other neurons. The synapses secrete an electrochemical neurotransmitter to the dendrites which have an excitatory or inhibitory influence on the firing of the neurons they connect to. Thus, each oscillator of the Kuromoto model can be seen as corresponding to the natural firing rate of a neuron. In order to make this model more realistic, different groups adapted the model and developed more sophisticated versions to provide different coupling strengths and time varying parameters [67].

To summarise, the population description might help to identify parts of the brain that belong to the seizure triggering zone. Since the mean field models remain relatively simple and deal with macroscale variables, they also represent the best physiological description of a seizure. These models are composed of a relatively small number of equations which makes computational simulations easy. The main disadvantage of these models is that they fail to suggest molecular and cellular mechanism of epileptogenesis and hence are unable to model therapeutics targeting molecular pathways responsible for seizures.

### A.3.2 Biophysical network models

These models provide a different approach by describing the brain from a microscopic scale [68]. Typically, they range from a single synapse to networks of millions of neurons. These models prove useful in investigating the role of biophysical and molecular properties of single neuron and neuronal networks in causing seizure like patterns of activity. Hence, these models are able to describe a finer scale of epilepsy at the molecular level and resulted in suggestions for therapeutic treatments based on results. The models are

initially calibrated to reproduce the experimentally observed properties of neuronal networks. Following this, the models are used to investigate the effect of various factors on the behavior of the network.

These models are designed to allow us to study the effect of factors that are usually inaccessible through experimental means. Their usefulness lies in investigating the different oscillatory behaviors that occur in the brain, before and during a seizure.

Viewing the brain from the microscopic level results in high dimensional systems and computationally expensive models. They also have an added uncertainty arising from the unknown processes on these spatial and temporal scales. Hence, results need a robust statistical analysis. Despite this, many researchers see this approach as one of the most useful in computational epilepsy [69].

Traub et al. [70, 71] provide extensive reviews of these models. To date, computational modelling combined with well designed experiments are a unique method for investigating the origins of epilepsy and also gives the opportunity to explore the oscillatory behavior of the brain and characteristic frequencies.

## A.4 Summary

We have chronologically reviewed different approaches that aid the understanding of epilepsy. Initially we reviewed the most common non-parametric methods. The nature of the brain is such that nonlinear methods seem to capture the dynamics of the system. However, much research has univariate measurements which fail to describe the synchronisation of neurons. Hence, it is unrealistic to assume that these measurements have a predictive power. Instead, multivariate and nonlinear variables together with robust statistical analysis provide a basis for more powerful algorithms for seizure prediction.

It is difficult to advance to models of seizure prediction without first under-

standing the underlying mechanisms of the brain. One way of advancing the understanding of brain dynamics is to use robust statistical analysis. Alternatively, we can model the dynamics of the brain using deterministic, computational or stochastic models. In this context, we reviewed some parametric models that have been able to unveil the unknowns of epilepsy and brain activity. Due to several experimental and clinical observations, the modelling work spans from the single synapse to networks of neurons, and from population models with two variables to detailed biophysical models involving tens of thousands of variables and parameters.

We discussed relatively simple mean field models and showed how these models could explain various EEG signals recorded during seizures and interictal to ictal transitions. We then moved into the detailed biophysical models and reviewed the most obvious advantages and limitations of each approach. We find that while biophysical network models are best suited for understanding the molecular and cellular bases of epilepsy, macroscopic models are more appropriate for describing epileptic processes occurring on large scale without having to consider the biophysical properties and hence, focusing on the purely dynamical aspects.

To address some of the limitations of each of these modelling methods the two approaches can be used as an 'across scale' approach. In this case relationships between variables on a cellular scale (from biophysical models) and aggregated parameters or variables governing the macroscopic models need to be established.

Another important category of computer models are not addressed in this report and can be directed towards the prediction of seizure onset and are well reviewed [51]. The advantage of stochastic modelling is that we can use observations to create noise models that implement a deterministic model ensuring we are capturing all the brain activity variability and not only the part of the signal that we are able to understand theoretically.

Despite an extraordinary amount of interest in understanding the dynamics of seizures, we still lack the understanding of the fundamental mechanisms

that govern this illness. The extensive variety of human epilepsies makes the quest for unifying principles especially difficult and perhaps a first goal would be to find predictive techniques for each patient and obtain more general results in future.

# B John Boland and Kathryn Ward: Hidden Markov models and change point estimation

Following on from the discussion in Section 4.2.1 the other method that is canvassed is the sample autocorrelation function (SACF) estimated using a moving window. As explained below, the SACF slowly decays and how slowly the decay ensues is an indication of the strength of linear correlation within the series. There is a conjecture that as a seizure becomes more imminent, the autocorrelation increases in strength [72].

## B.1 Hidden Markov models

Consider a system (see Figure 4) where you observe the grass on your front lawn (adapted from [73]). Some days the grass will be wet, and other days it will be dry. If the grass is wet, there are two possible reasons: either it rained or you have left a sprinkler on. You do not know which one is the correct reason for your grass being wet (the hidden causation process), all you can observe is that the grass is wet. Over a series of days you may be able to make a prediction about the reason for your grass being wet. If you observe a series of days where your grass has been dry, followed by one wet day, you may find that you have left your sprinkler on over night. However, if you find that the grass is wet over a number of days, you may suspect that it has been raining. Over a period of time you can thus build up a probability

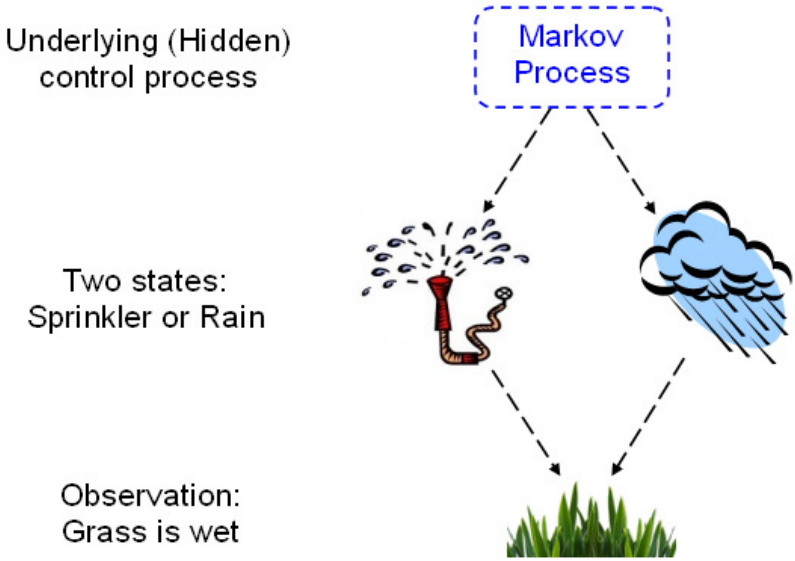


FIGURE 4: Pictorially, a Hidden Markov model where the state of the grass (wet or dry) is observed, but the cause of the state (either the sprinkler or rain) is unknown.

profile which estimates the probability of being in each state, given the known history.

Now, consider the case that instead of just observing that the grass is wet, you can now measure how much water has gone into the soil; from zero millimeters to an infinite number of millimeters. Now our observations can have an infinite number of realisations, but we still have two possible reasons for the grass (or soil) being wet. We can estimate the probability profile for this system.

## B.2 Theory of hidden Markov models

We now consider hidden Markov model theory [32]. Consider a process $X$ with a time parameter set of $\{0, 1, 2, \ldots\}$. Suppose $X$ has a general finite state space $S = \{s_1, s_2, \ldots, s_N\}$. Without loss of generality we rewrite the elements of $S$ as the standard unit vectors so that $S = \{e_1, e_2, \ldots, e_N\}$ where $e_i = (0, \ldots, 0, 1, 0, \ldots, 0)$ [32].

Let $\mathcal{F}_k = \sigma(X_0, X_1, \ldots, X_k)$ be the history of the Markov chain up to the current time $k$. The Markov property of our states is thus that the probability of being in state $j$ at time $k+1$, given all of the history of the chain, is equal to the probability of being in state $j$ at time $k+1$ given the previous state:

$$\Pr(X_{k+1} = e_j \mid \mathcal{F}_k) = \Pr(X_{k+1} = e_j \mid X_k). \tag{2}$$

Let $A$ be the transition matrix of the Markov chain, where $a_{ij}$ is the probability of transiting to state $i$ given that the current state is $j$. Then it can be shown that [32]

$$\begin{aligned} \mathrm{E}\left[X_{k+1} \mid X_k\right] &= \sum_{i=1}^{N} \mathrm{E}\left[X_{k+1} \mid X_k = e_i\right] \langle X_k, e_i \rangle \\ &= \sum_{i=1}^{n} \sum_{j=1}^{N} \mathrm{E}\left[\langle X_{k+1}, e_j \rangle \mid X_k = e_i\right] \langle X_k, e_i \rangle \, e_j \end{aligned}$$

$$= \sum_{i=1}^{n} \sum_{j=1}^{N} a_{ji} \langle X_k, e_i \rangle e_j$$
$$= AX_k . \quad (3)$$

Here $\langle a, b \rangle$ is the inner product of two vectors $a$ and $b$.

Let us define $V_{k+1} = X_{k+1} - AX_k$ as the martingale noise associated with moving from state $X_k$ to state $X_{k+1}$. Then

$$X_{k+1} = AX_k + V_{k+1} . \quad (4)$$

As discussed by Elliott et al. [32, Chapter 3], suppose that we cannot observe $X$ directly, but that we do observe a real world series $y$ such that

$$y_{k+1} = c(X_k) + \sigma(X_k) w_{k+1} , \quad k = 0, 1, 2, \ldots , \quad (5)$$

where $\{w_k\}$ are individually and identically distributed random variables which are independent of $X$. Both $c$ and $\sigma$ are real functions of $X$ which are identified with vectors $(c_1, \ldots, c_N)$ and $(\sigma_1, \ldots, \sigma_N)$ such that $c(X_k) = \langle c, X_k \rangle$ and $\sigma(X_k) = \langle \sigma, X_k \rangle$.

The hidden Markov model is a reflection that the Markov chain $X$ is not directly observed but is hidden in the 'noisy' $y$ observations. Recall that $\mathcal{F}_k = \{X_0, \ldots, X_k\}$ represents the history of the Markov chain $X$, and let $\mathcal{Y}_k = \{y_1, \ldots, y_k\}$ represent the history of Markov chain $Y$, and represent the joined chains by $\mathcal{G}_k = \{X_0, \ldots, X_k, y_1, \ldots, y_k\}$. These are known as the filtrations representing the histories of the respective state processes.

### B.2.1 Changing the measure

Under the configuration in Section B.2, it can be very difficult to estimate the transition probabilities $a_{ij}$ as well as the variability $\sigma$. We now change the measure we are working under, in order to make these estimations simpler.

Assume [32] that under some probability measure $\overline{P}$, $y$ is a sequence of independent and identically distributed random variables such that $y_k \sim N(0,1)$ for all $k$. Under $\overline{P}$, $X$ is a Markov chain that is independent of $Y$ with state space $S = \{e_1, \ldots, e_N\}$ and transition matrix $A = (a_{ij})$ such as in Equation (4), and $\overline{E}[V_{k+1} \mid \mathcal{G}_k] = \overline{E}[V_{k+1} \mid \mathcal{F}_k] = \overline{E}[V_{k+1} \mid X_k] = 0 \in R^N$.

Define [32]

$$\overline{\lambda_\ell} = \frac{\phi\left(\langle \sigma, X_{\ell-1}\rangle^{-1}\left(y_i - \langle c, X_{\ell-1}\rangle\right)\right)}{\langle \sigma, X_{\ell-1}\rangle\, \phi(y_i)}, \tag{6}$$

$$\overline{\Lambda_k} = \prod_{\ell-1}^{k} \overline{\lambda_\ell}, \quad k \geqslant 1, \tag{7}$$

where $\phi(x)$ is the standard normal density.

As shown by Elliott et al. [32, Chapter 3] a new probability measure $P$ is defined using the Radon–Nikodyn derivative [74] such that

$$\left.\frac{dP}{d\overline{P}}\right|_{\mathcal{G}_k} = \overline{\Lambda}_k\,. \tag{8}$$

Under $P$, $X$ is a Markov chain with transition matrix $A$ and $\Pr(Y_{k+1} = f_j \mid X_k = e_i) = c_{ji}$. That is,

$$X_{k+1} = AX_k + V_{k+1}\,, \tag{9}$$

$$y_{k+1} = \langle c, X_k\rangle + \langle \sigma, X_k\rangle\, w_{k+1}\,, \tag{10}$$

so $P$ is the measure used in the original formulation (in B.2). Note [32]: $\overline{P}$ is a better framework to work within because each element is estimated more easily.

### B.2.2 Updating estimates as new observations arrive

The parameters of this model are the transition matrix $A = (a_{ji})$ and the functions $c = (c_i)$ and $\sigma = (\sigma_i)$. We use estimates of the following processes

to estimate these parameters:

$$\begin{aligned} J_k^{ij} &= \text{the number of jumps from state } i \text{ to state } j \text{ in time } k \\ &= \sum_{n=1}^{k} \langle X_{n-1}, e_i \rangle \langle X_n, e_j \rangle , \qquad (11) \\ O_k^i &= \text{the amount of time } X \text{ has spent in state } i \text{ up to time } k \\ &= \sum_{n=1}^{k} \langle X_{n-1}, e_i \rangle , \qquad (12) \\ T_k^i(f) &= \text{the amount of time } X \text{ has spent in state } i \text{ up to time } k \\ &\quad \text{weighted by a the observations } y_n. \\ &= \sum_{n=1}^{k} \langle X_{n-1}, e_i \rangle f(y_n), \qquad (13) \end{aligned}$$

where either $f(y) = y$ or $f(y) = y^2$.

Suppose we observe $y_1, \ldots, y_k$. We wish to obtain estimates for $X_0, X_1, \ldots, X_k$. The best mean square estimate of $X_k$ given $\mathcal{Y}_k = \sigma\{Y_1, \ldots, Y_k\}$ is

$$E[X_k \mid \mathcal{Y}_k] \in R^N, \qquad (14)$$

which is often difficult to calculate. However, working under $\overline{P}$,

$$E[X_k \mid \mathcal{Y}_k] = \frac{\overline{E}[\overline{\Lambda}_k X_k \mid \mathcal{Y}_k]}{\overline{E}[\overline{\Lambda}_k \mid \mathcal{Y}_k]} . \qquad (15)$$

Let $q_k := \overline{E}[\overline{\Lambda}_k X_k \mid \mathcal{Y}_k] \in R^N$ be the unnormalised conditional expectation of $X_k$ given the history of $Y$. Now, $\sum_{i=1}^{N} \langle X_k, e_i \rangle = 1$ and with $\mathbf{1} = (1, 1, \ldots, 1) \in R^N$ (where $\langle \mathbf{a}, \mathbf{b} \rangle$ is the inner product of the two vectors $a$ and $b$),

$$E[X_k \mid \mathcal{Y}_k] = \frac{q_k}{\langle q_k, \mathbf{1} \rangle} . \qquad (16)$$

With entries $\phi\left[\sigma_i^{-1}(y_{k+1}-c_i)\right]/\left[\sigma_i\phi(y_k+1)\right]$, $B(y_{k+1})$ is a diagonal matrix. Then the recursive dynamics of the processes defined above are [32]:

$$\begin{aligned}
\sigma(J^{ij}X)_{k+1} &= AB(y_{k+1})\sigma(J^{ij}X)_k && (17)\\
&\quad + \langle q_k, e_i\rangle \frac{\phi\left(\sigma_i^{-1}(y_{k+1}-c_i)\right)}{\sigma_i\phi(y_{k+1})} a_{ji}e_j\,, && (18)\\
\sigma(O^iX)_{k+1} &= AB(y_{k+1})\sigma(O^iX)_k && (19)\\
&\quad + \langle q_k, e_i\rangle \frac{\phi\left(\sigma_i^{-1}(y_{k+1}-c_i)\right)}{\sigma_i\phi(y_{k+1})} Ae_i\,, && (20)\\
\sigma(T^i(f)X)_{k+1} &= AB(y_{k+1})\sigma(T^i(f)X)_k && (21)\\
&\quad + \langle q_k, e_i\rangle \frac{\phi\left(\sigma_i^{-1}(y_{k+1}-c_i)\right)}{\sigma_i\phi(y_{k+1})} f(y_{k+1})Ae_i\,, && (22)\\
q_{k+1} &= AB(y_{k+1})q_k\,. && (23)
\end{aligned}$$

The estimates for the entries of the transition matrix $A$ are

$$\hat{a}_{ji} = \frac{\hat{J}_k^{ij}}{\hat{O}_k^i} = \frac{\sigma(J^{ij})_k}{\sigma(O^i)_k}\,, \tag{24}$$

and

$$\hat{c}_i = \frac{\hat{T}_k^i(y)}{\hat{O}_k^i} = \frac{\sigma(T^i(y))_k}{\sigma(O^i)_k}\,, \tag{25}$$

$$\hat{\sigma}_i = \left\{\left[\hat{T}_k^i(y^2) - 2c_i\hat{T}_k^i(y) + c_i^2\hat{O}_k^i\right]/\hat{O}_k^i\right\}^{1/2}. \tag{26}$$

## B.3 Change point estimation

We describe two methods of estimating change points in time series. They are indicative of a switch in the process generating the time series. Thus they can be important indicators of changes in the condition of the patient [72].

### B.3.1 Exponentially smoothed forecast variance

One potential indicator of a change point discussed by Mormann et al. [53] is a change in variance of the series. One can estimate the variance of a time series by calculating the moving average and then moving variance with a moving window of some specified length. Alternatively, we would suggest that a better indicator of a change point is the estimate of the exponentially smoothed forecast variance. The advantage to this version is that the most recent values of the series are more highly weighted than values in the distant past. We estimate this forecast variance as [75]

$$\tilde{V}(t) = \beta(X(t) - \bar{X}(t-1))^2 + (1-\beta)\tilde{V}(t-1), \tag{27}$$

where

$$\bar{X}(t-1) = \alpha X(t) + (1-\alpha)\bar{X}(t-1), \tag{28}$$

with $X(t)$ the value of the series at time $t$, and $\alpha, \beta \in (0,1)$ are smoothing parameters. In general the values for $\alpha$ considered appropriate are between $0.01$ and $0.3$. A heuristic for selecting $\beta$ is $\beta^* = 0.043 - 0.01\alpha^*$.

### B.3.2 Sample autocorrelation function

Mormann et al. [53] also describe an aspect of the autocorrelation function of a series as an indicator of change point. The sample autocorrelation function is defined by

$$A(\tau) = \frac{1}{(n-1)\hat{\sigma}^2} \sum_{i=1}^{n-\tau} x_i x_{i-\tau}\,, \tag{29}$$

where $\hat{\sigma}^2$ is the estimate of the long range variance.

The sample autocorrelation decays from $A(0)$ as $\tau$ increases and fluctuates around zero for large $\tau$. The slower $A(\tau)$ decays the stronger are the linear correlations of the series. If we estimate $A(\tau)$ with a moving window and estimate the first zero crossing of it, we can see how the strength of the

linear correlation changes. The conjecture is that as a seizure approaches, the strength of the autocorrelation will increase. The first zero crossing is defined as

$$\tau_0 = \min\{\tau \mid A(\tau) = 0\}. \tag{30}$$

## B.4 Conclusion

Two main determinations with respect to an EEG trace are:

1. Is one able to identify how many states of the system the trace describes?
2. How can one identify a switch from one state to another?

We presented methods by which the presenters of this problem can begin to answer these questions.

# C Burzin Bhavnagri: Analyzing EEG and fMRI data for sudden changes or discontinuities

At the 2010 MISG at RMIT, the following problem was posed by Abbott, Masterton, Jackson and collaborators, which relates to the Brain Research Institutes research into epilepsy. Data are collected as ElectroEncephelogGram (EEG). Initially, the potential $P(x_i, y_j, t_k)$ is measured at various locations $x_i$, $y_j$ on the patients scalp at various times $t_k$. For each $t_k$, the potential differences $V$ are evaluated between the values of $P$ at $x_i$, $y_j$ and the other locations $x_{i'}$, $y_{j'}$ on the patient's scalp. The full set of potential differences for all the time points $t_k$ and all possible pairing of the locations on the scalp form the EEG data $V$ and are stored as a family of time series, as shown in Figure 1.

If, during the recording of the EEG, the patient has an epileptic event or seizure, then, as illustrated in Figure 1, there is a distinct change, 'discontinuity', in the structure within the EEG data $\mathsf{V}$. As explained in Appendix A, the difficulty with the EEG data is that it only sees activity in cortex (the surface outer regions of the brain), whereas the initiation of an epileptic episode is believed to occur deep within the brain.

A patient can simultaneously or separately have a functional magnetic resonance (fMRI) scan from which information about the blood oxygenation level dependent (BOLD) activity deep within the brain can be recovered; namely, $\mathsf{F}(\mathsf{x}_l, \mathsf{y}_m, \mathsf{z}_n, \mathsf{t}_r)$, where the $\mathsf{x}_l$, $\mathsf{y}_m$, $\mathsf{z}_n$ denote the voxels in the reconstructed three dimensional image of the brain activity at various times $\mathsf{t}_r$. The fMRI scans often reveal changes which spread out from single or multiple focal points, depending on the type of epilepsy. If the focal area is identified, it may be amenable to surgical treatment.

The consequential challenge is whether, when 'discontinuities' are observed in the values of the EEG data $\mathsf{V}$, earlier 'discontinuities' have occurred in some of the voxels of the fMRI data $\mathsf{F}$. Thus, a key aim in the utilisation of fMRI data is the determination of if, when and where a cascade of abnormal activity starts within the brain prior to the observation of 'discontinuities' in the EEG data associated with an epileptic event/siezure.

One possible way of performing the 'if, when and where' determination is to utilise recent research that exploits that a smooth non-vanishing vector field on a smooth manifold has integral curves that never intersect themselves or each other [33]. Discontinuities of two dimensional functions defined on a plane can be found and analysed using some of the theorems by Bhavnagri [33]. Such procedures, via principal component analysis or independent component analysis, are applied directly to the fMRI data.

Initially, we consider the direct application of such procedures. The first step is the definition of the various two dimensional functions to be analysed. This can be achieved in different ways, because the functions $\mathsf{V}$ and $\mathsf{F}$ are functions of three and four variables, respectively. One possibility is to simply fix some

of the variables. Some representative examples include

$$\begin{aligned} V(x_i, y_j, t_k) &\mapsto V_{1j}(x_i, t_k), \\ V(x_i, y_j, t_k) &\mapsto V_{2i}(y_j, t_k), \\ F(x_l, y_m, z_n, t_r) &\mapsto F_{nr}(x_l, y_m), \end{aligned}$$

where $y_j$ has been fixed in the first example, $x_i$ in the second, and $z_n$ and $t_r$ in the third. Alternatively, various forms of averaging could be applied with respect to the variables that are chosen to be fixed. A moving average is used by many authors on epilepsy data, for example to correct artifacts in EEG or fMRI data [76, 77].

Because of the numerous ways in which this could be done, the following notation is introduced to denote the particular two dimensional form chosen for $V$ or $F$: $V_\theta(x, y)$ or $F_{\theta,\phi}(x, y)$, where $\theta$ and $\phi$ denote the variables that have been fixed and $x$, $y$ the coordinates in the plane.

As mentioned above, the theory is based on the observation that a smooth non-vanishing vector field on a smooth manifold has integral curves that never intersect themselves or each other. Bhavnagri [33] provided simpler and more direct discussion than that of the original [34]. It is a direct corollary of the theory that singularities are found by identifying 'if and where' such curves intersect themselves or each other. A key step is the choice of the vector field. For the chosen $V_\theta(x, y)$ or $F_{\theta,\phi}(x, y)$, an operator like $-\frac{\partial}{\partial y}$ or $\frac{\partial}{\partial x}$ can be applied. It is a convenient choice for two reasons. Firstly, it is a Hamiltonian operator and that has integral curves $V_\theta(x, y) =$ constant or $F_{\theta,\phi}(x, y) =$ constant with $(x, y)$ denoting the points along the integral curves. This circumvents errors associated with numerical differentiation, numerical equation solving, and even floating point arithmetic.

The non-vanishing is a crucial condition in the theory, as shown by the example of a saddle function like $F_{\theta,\phi}(x, y) = x^2 - y^2$. The level curves are shown below the saddle in Figure 5, notice the two straight lines intersect at the origin. However, the saddle is certainly smooth. The Hamiltonian field vanishes at the origin. If we look at a vector along the integral curves, as we

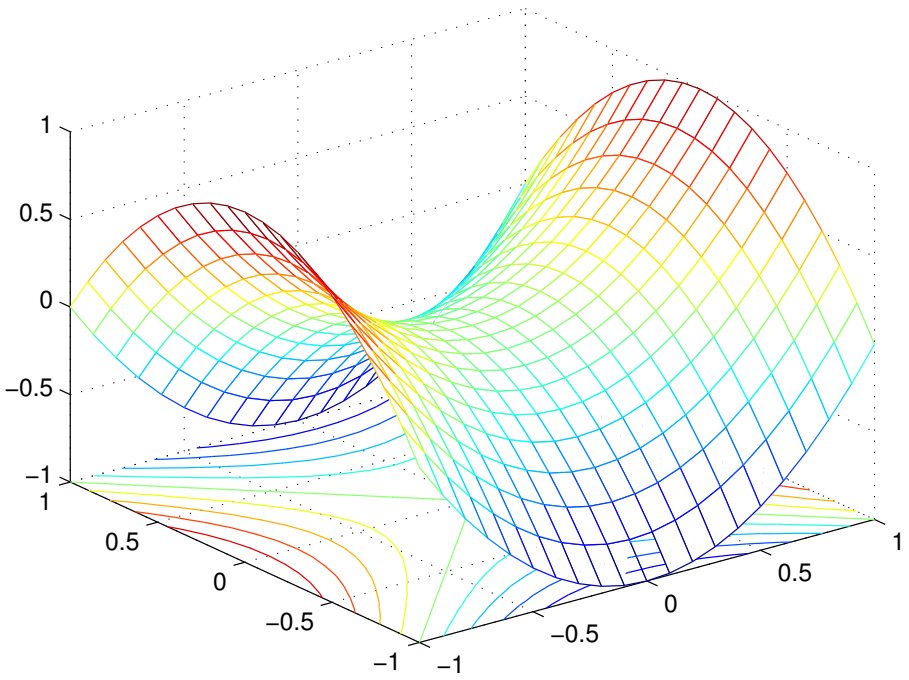


FIGURE 5: Saddle shaped section of EEG $V$ or fMRI $F$.

get closer to the origin, the vectors keep getting smaller and smaller. It is only intersecting integral curves where the Hamiltonian field does not vanish that are of interest.

Since this non-vanishing condition is important it is built into the algorithm. One case is that the Hamiltonian vanishes when $V_\theta(x, y) = \text{constant}$ or $F_{\theta,\phi}(x, y) = \text{constant}$ in a neighborhood instead of along a curve in which case

$$\frac{\partial V_\theta}{\partial x} = 0 = \frac{\partial V_\theta}{\partial y},$$

or alternatively the same equation with $F_{\theta,\phi}$ instead of $V_\theta$. In this case no conclusion can be drawn and perhaps a different $\theta$ for EEG or $\theta$, $\phi$ for fMRI would be a better choice.

To exclude constant neighborhoods in our $\theta$ or $\theta$, $\phi$ slice we approximate $V_\theta(x, y) = \text{constant}$ or $F_{\theta,\phi}(x, y) = \text{constant}$ with the boundary of that subset where $V_\theta$ or $F_{\theta,\phi}$ is less than the constant

$$V_c = \partial\{(x, y) \mid V_\theta(x, y) < c\},$$
$$F_c = \partial\{(x, y) \mid F_{\theta,\phi}(x, y) < c\}.$$

This produces curves and avoids the exceptional cases.

Theory shows the discontinuity problem can be reduced to calculating intersections of certain curves. With the choice of Hamiltonian, and using the boundaries instead of levels as above, this is characterised by the three inequalities below [33]. Two sets $V_c$ and $V_d$ for $c \neq d$ intersect at a point $(x, y)$ if and only if there exist two neighbouring points $(x', y')$ and $(x'', y'')$ and two thresholds $\varepsilon > 0$ and $\varepsilon' > 0$ such that

$$\begin{aligned} V_\theta(x, y) - V_\theta(x', y') &\geqslant \varepsilon, \\ V_\theta(x, y) - V_\theta(x'', y'') &\geqslant \varepsilon', \\ \varepsilon + V_\theta(x', y') &\neq \varepsilon' + V_\theta(x'', y''). \end{aligned}$$

Likewise for $F_{\theta,\phi}$ the choice of Hamiltonian reduces the problem to three inequalities.

This is an interesting way of finding discontinuities, there is a need to extend it further for reasons such as

- in epilepsy data as in other imaging data there is much noise superimposed on the signal, and
- discontinuity detection is a point based analysis, but in many applications like epilepsy diagnosis a region is sought, such as for surgery.

These are both statistical problems so we suggest an interesting statistic $\lambda_{ij}/\Delta_{ij}$ where

$$\Delta_{ij} = (x_{i+1} - x_i)(y_{j+1} - y_j) - (x_{j+1} - x_j)(y_{i+1} - y_i),$$
$$\lambda_{ij} = (y_{j+1} - y_j)(x_j - x_i) - (x_{j+1} - x_j)(y_j - y_i).$$

and $(x_i, y_i), (x_{i+1}, y_{i+1}) \in V_c$ and $(x_j, y_j), (x_{j+1}, y_{j+1}) \in V_d$, or $F_c$ and $F_d$ respectively, with $c \neq d$, where $F_c$ is the boundary of that subset where $F_{\theta,\phi}$ is less than $c$ ($F_c$ is defined above) and $F_d$ is the boundary of that subset where $F_{\theta,\phi}$ is less than $d$ by applying the same notation with $d$ instead of $c$. Here the $i$th and $(i+1)$th points belongs to one set approximating an integral curve, and the $j$th and $(j+1)$th points belong to the other. Consider the line joining points $(x_i, y_i)$ and $(x_{i+1}, y_{i+1})$, its parametric equation is $\mathbf{p} = (x_i, y_i) + s(x_{i+1} - x_i, y_{i+1} - y_i)$. Likewise consider the line joining points $(x_j, y_j)$ and $(x_{j+1}, y_{j+1})$, its parametric equation is $\mathbf{p} = (x_j, y_j) + t(x_{j+1} - x_j, y_{j+1} - y_j)$. When the two lines are not parallel they have a unique point of intersection given by the matrix equation

$$\begin{bmatrix} x_{i+1} - x_i & x_{j+1} - x_j \\ y_{i+1} - y_i & y_{j+1} - y_j \end{bmatrix} \begin{bmatrix} s \\ t \end{bmatrix} = \begin{bmatrix} x_j - x_i \\ y_j - y_i \end{bmatrix}.$$

Now $\Delta_{ij}$ is the determinant of the $2 \times 2$ matrix above; inverting this matrix we find that $s = \lambda_{ij}/\Delta_{ij}$ and $t = \lambda_{ji}/\Delta_{ij}$ are coordinates of the intersection of the two lines. Furthermore the sign of $\Delta_{i(i+1)}$ for each vertex $i$ defines what is called a binary string descriptor for a simple closed non-degenerate polygon [35].

The $i$th edge intersects the $j$th edge if and only if

$$\lambda_{ij}/\Delta_{ij} \in [0, 1] \quad \text{and} \quad \lambda_{ji}/\Delta_{ji} \in [0, 1]$$

due to the parametrisation chosen. So this provides a statistic for discontinuity in the presence of noise. The advantage being amenability to further statistical analysis.

Perhaps numerical methods have much relevance to detecting more discontinuities than the choice of Hamiltonian, although convenient, can detect. Moreover the theory shows a huge range of transformations can be performed to the data $V_\theta$ or $F_{\theta,\phi}$. All that is required is that the transformation be smooth. The PCA and ICA are particularly interesting candidates for this role, as it has been observed that the dimensionality of the EEG signal may fall before an epileptic seizure [72].

Since the theory shows a huge range of transformations can be performed to the data $V_\theta$ or $F_{\theta,\phi}$ it seems natural to look for a way of classifying transformations. A foliation is a useful generalisation of an integral curve. In non-commutative geometry foliations are canonically associated with a Von Neumann algebra [78]. Two foliations with the same leaf space have isomorphic von Neumann algebras. Foliations can be classified by the type of their associated Von Neumann algebra, either type I, II or III. Murray and Von Neumann classified the Von Neumann algebras using the notion of a factor. A factor is a Von Neumann algebra whose center reduces to $\mathbf{C}$. The complete list of factors is $I_n$, $I_\infty$, $II_1$, $II_\infty$, $III_\lambda$, $III_1$ and $III_0$. The Reeb foliation is an example of type I. The Kronecker foliation is an example of type $II_\infty$. A particularly interesting example of Von Neumann algebra of type $II_\infty$ was found by Carey, Phillips and Evans [79, 80].

# D Mali Abdollahian, S. Zahra Hosseinifard and Nahid Jafariasbagh: Profile monitoring for brain activities using fMRI data to locate the onset of seizure

Following on from Section 4.2.3, this appendix analyzes in greater detail the appropriateness of profile monitoring as a tool for seizure prediction. Profile monitoring is the use of control charts for cases in which the quality

of a process or product can be characterised by a functional relationship between a response variable and one or more explanatory variables. For example, to estimate the dose-response curve of a manufactured drug, once a batch of the drug is produced, several doses of the drug are administered to patients and the responses are measured. The resultant dose-response curve summarises the quality of the particular batch of the drug, indicating the maximal effective response, minimal effective response, and the rate in which the response change between the two [81]. Another example of a process characterised by a profile is a semiconductor manufacturing quality control problem involving calibration in which the performance of the mass flow controller is monitored by a linear function [82]. As profile monitoring falls under the broad field of functional data analysis, Ramsay and Silverman [83] discussed various examples of functional data or profiles. Mahmoud et al. [84] presented a method to detect change points in linear profile monitoring using segmented regression technique. Some researchers used different terminologies to express the profile. Gardner et al. [85] applied the term 'signature' in their study whereas Jin and Shi [86, 87] used the term 'waveform signals'.

Different control charts have been proposed for profile monitoring, of which some are univariate such as Shewhart, cumulative SUM (CUSUM) and exponentially weighted moving average (EWMA), and some such as, multi cusum (MCUSUM) and multi EWMA (MEWMA) are multivariate. Multivariate charts can monitor more than one correlated quality characteristics simultaneously. The EWMA chart is used extensively in time series modelling and in forecasting [88]. Therefore, here we propose an EWMA chart for monitoring the performance of the profile fitted to the brain activities of epileptic patients. Sections D.2 and D.3 explain the reasons for this proposal.

It is known that fMRI measures the changes in blood oxygenation. Previous studies modelled the blood changes as a convolution of the EEG discharges with a canonical hemodynamic response function in the general linear model framework [89]. Also, fMRI measurements can be modelled by a mathematical function in $\mathfrak{n}$ dimensional space [90, 91, 92, 81, 93]. Here we model the change in blood oxygenation (measured by fMRI) as a function of the EEG discharge.

For simplicity we assume that this model (profile) is known. Our aim is to use $\frac{2}{3}$ of available fMRI data to build an appropriate profile model and use the remaining $\frac{1}{3}$ of data to assess the validity of the model.

## D.1 Methodology

To explain the methodology, let us assume that brain activities are represented by the simple linear regression function

$$Y(i) = X\beta(i) + \sigma(i)\epsilon(i)\,, \tag{31}$$

where $Y(i)$ is a column vector of $n$ observations at point $i$, $X$ is a design matrix incorporating the response to the task (common to all points), $\beta(i)$ is a column vector of unknown coefficients, $\sigma(i)$ is an unknown scalar standard deviation, and $\epsilon(i)$ is a column vector of temporally correlated Gaussian errors.

Profile monitoring assumes that for each profile ($j > 1$) the $j$th value of the response variable $Y$ is measured along with the corresponding values of one or more explanatory variables $X$, reflecting the location of the measurement on a process.

As a general case, assume that $X_1, X_2, \ldots, X_{p-1}$ and $Y$ are the variables in a linear profile, represented by Equation (33), where $Y$ is the quality characteristic under the study (e.g. brain activity), $X$ are the explanatory variables, the indices $j$ and $i$ are the sample number and the observation within the sample respectively. Moreover, the random variables $\epsilon_{ij}$ (called residuals) are independent and normally distributed with mean zero and variance $\sigma^2$:

$$\begin{aligned} &Y_{ij} = \beta_0 + \beta_1 X_{1,ij} + \beta_2 X_{2,ij} + \cdots + \beta_{p-1} X_{p-1,ij} + \epsilon_{ij}\,, \\ &i = 1, 2, \ldots, n\,, \quad j = 1, 2, \ldots, m\,. \end{aligned} \tag{32}$$

For the simplest case consider the simple linear regression model:

$$Y_{ij} = \beta_0 + \beta_1 X_{1,ij} + \epsilon_{ij}\,, \quad i = 1, 2, \ldots, n\,, \quad j = 1, 2, \ldots, m\,. \tag{33}$$

In phase I of linear profile we establish the reference line (reference model) when the parameters of the process are unknown [82]. Therefore, the estimated linear regression function (mathematical model) based on all available in-control data is

$$\hat{Y} = b_0 + b_1 X_1 . \tag{34}$$

Where $b_0$ and $b_1$ are the least square estimates of $\beta_0$ and $\beta_1$, respectively. When the usual assumptions hold the estimators $b_0$ and $b_1$ are normally distributed random variables with mean $\beta_0$ and $\beta_1$, respectively [94]. The least square estimators of regression coefficients in Phase I for sample $j$ are [95]

$$\begin{aligned} b_{0j} &= \bar{y}_j - b_{1j}\bar{x}, \quad j = 1, 2, \ldots, k, \\ b_{1j} &= \frac{\sum_{i=1}^{n} y_{ij}(x_i - \bar{x})}{\sum_{i=1}^{n}(x_i - \bar{x})^2}, \end{aligned} \tag{35}$$

where $\bar{y}_j = \frac{1}{n}\sum_{i=1}^{n} y_{ij}$, $\bar{x} = \frac{1}{n}\sum_{i=1}^{n} x_i$. The sample statistics $b_{0j}$ and $b_{1j}$ have a bivariate distribution with the mean vector $\mu = (\beta_0, \beta_1)$ and the variance/covariance matrix

$$\Sigma = \begin{bmatrix} \sigma_0^2 & \sigma_{01}^2 \\ \sigma_{01}^2 & \sigma_1^2 \end{bmatrix}. \tag{36}$$

Where

$$\begin{aligned} \sigma_0^2 &= \sigma^2 \left[ \frac{1}{n} + \frac{1}{\sum_{i=1}^{n}(x_i - \bar{x})^2} \right], \\ \sigma_1^2 &= \frac{-\sigma^2}{\sum_{i=1}^{n}(x_i - \bar{x})^2}, \\ \sigma_{01}^2 &= -\sigma^2 \frac{\bar{x}}{\sum_{i=1}^{n}(x_i - \bar{x})^2}, \end{aligned}$$

are the variance of $b_{0j}$ and $b_{1j}$ and the covariance between $b_{0j}$ and $b_{1j}$ and respectively. This joint distribution is bivariate normal distribution when the residual follows a normal distribution. The estimate of $\beta_0$ and $\beta_1$ and $\sigma_0^2$ are

$$b_0 = \frac{\sum_{j=1}^{k} b_{0j}}{k}, \quad b_1 = \frac{\sum_{j=1}^{k} b_{1j}}{k}, \quad \text{MSE} = \frac{\sum_{j=1}^{k} \text{MSE}_j}{k}. \tag{37}$$

where

$$\text{MSE}_j = \frac{\sum_{i=1}^{n} e_{ij}^2}{n-2} \tag{38}$$

is the unbiased estimator of $\sigma_0^2$ for sample $j$, and

$$e_{ij} = y_{ij} - \hat{y}_{ij} \tag{39}$$

where $\hat{y}_{ij}$ is a fitted value. After determining the initial estimates of the regression parameters as given in Equation (37), Kang and Albin [95] advised using these estimates to calculate control limits.

We propose to collect the control data when the patient is in normal condition (no seizure) or use the data of a normal person (depending on the advice from medical practitioners in the field). We will then calculate $b_0$ and $b_1$ based on the in control data. This is called Phase I of process monitoring. The purpose of Phase II analysis is to quickly detect any shift in the values of the in-control parameters estimated in Phase I. Often these parameters are correlated, therefore we would employ multivariate profile monitoring charts to simultaneously monitor the changes in all the parameters [96, 97, 98]. In Phase II, one compares the competing methods in terms of their corresponding run length distribution, where the run length is defined as the number of samples taken until out-of-control signal is given. In the next section we discuss the theory and properties of EWMA chart and provide reasons for selecting this chart to monitor brain activities.

## D.2 The EWMA/R control charts

In EWMA control chart, the $t$th value of the control response, $z_t$ which is plotted in the chart, is the weighted average of the $t$th residual average, $\bar{e}_t = n^{-1} \sum_{i=1}^{n} e_{it}$ , and the value of $z_{t-1}$:

$$z_t = (1-\theta) z_{t-1} + \theta \bar{e}_t \,, \tag{40}$$

where $0 < \theta \leqslant 1$ is the weighting constant and $z_0 = 0$.

We rewrite Equation (40) as

$$z_t = \theta\bar{y}_t + (1-\theta)z_{t-1} = z_{t-1} + \theta(\bar{y}_t - z_{t-1})\,, \tag{41}$$

where $z_{t-1}$ is forecast of $\bar{y}_t$ at time $t$, then $e_t = \bar{y}_t - z_{t-1}$ is the forecasted error at time $t$ and

$$z_t = z_{t-1} + \theta e_t\,. \tag{42}$$

In Equation (41), if we replace $z_{t-1}$ in terms of $z_{t-2}$ and $z_{t-2}$ in terms of $z_{t-3}$ and so on, we find that $z_t$ (the statistics plotted at time $t$ in EWMA chart) is a function of all the previous response values $\bar{y}_t$. The chart is sometimes referred to as a chart with memory. However, the dependency weight decreases as we move away from the starting samples. If it is desired to allocate more weight to the data collected prior to the current time, then we should select weight value closer to 0.0, say $\theta = 0.2$. On the other hand, if it is desired to allocate more weight towards the current sample response, then we should select weight value closer to 1.0, say $\theta = 0.8$ or 0.9.

The control limits for the EWMA chart are

$$LCL = -L\sigma\sqrt{\frac{\theta}{(2-\theta)n}} \quad \text{and} \quad UCL = +L\sigma\sqrt{\frac{\theta}{(2-\theta)n}}\,, \tag{43}$$

where $\sigma$ is the error term standard deviation estimated by $\sqrt{n^{-1}\sum_{j=1}^{n} MSE_j}$, $MSE_j$ is the mean square error of the $j$th fitted regression line. $L(>0)$ is the multiple of the sample statistic standard deviation that determines the false alarm rate, and $n$ is the sample size. Typical values are $L = 3$ and $\theta = 0.08$, 0.1, 0.15 or 0.2 [88]. If we select $L < 3$, then we over control the process. However, in some medical area we prefer to over control the data in order to avoid misdiagnosing the patient's condition. The value of $L$ is selected based on the medical practitioners stating how much change in the parameters of the control model would lead to a seizure. We may have to define a new mathematical model for the control limits.

EWMA charts are used extensively in time series modelling and forecasting. It is very insensitive to normality assumptions. Therefore it is an ideal chart for individual profile measurements.

## D.3 Properties of EWMA

EWMA chart can be optimised to detect small or large shifts in the parameters of the fitted profile (by adjusting $\theta$). It is also capable of forecasting the process profile for the next period; $z_t$ is a forecast of process profile at time $t+1$. Therefore it is very useful for a dynamic process algorithm. If the forecast is different from the recorded value of the response variable in the mathematical model, then an operator can make necessary adjustment to $\theta$. This section discusses how to increase the forecasting ability of EWMA chart by monitoring the forecast error and reducing it by optimizing the value of $\theta$.

## D.4 Improving the forecasting ability of the ewma chart

Rewrite Equation (41) as $z_t = z_{t-1} + \theta_t e_t + \theta_2 \sum_{j=1}^{t} e_t$ where $\theta_1$ and $\theta_2$ are constants that give weight to the error at time $t$ and the sum of the errors accumulated at time $t$. Let $\delta e_t$ be the first difference of the errors, then $z_t = z_{t-1} + \theta_t e_t + \theta_2 \sum_{j=1}^{t} e_j + \theta_3 \delta e_t$ where $\theta_1$ and $\theta_2$ are constants that give weight to the error at time $t$ and the sum of the errors accumulated at time $t$. Therefore, the forecasted response value at time $t+1$, $z_t$, equals the current value of profile response $\bar{y}_t$ plus the terms related to the errors. The ability of EWMA forecasting will greatly improve when we choose the optimal $\theta_1$, $\theta_2$ and $\theta_3$. In practice the EWMA statistics $z_t$ is often plotted one time period ahead together with the measurements of the current profile response $\bar{y}_t$. This allows the practitioner to observe the error of the forecast. In statistical profile monitoring applications where the profile response is a function of time, this approach has considerable appeal. The range or

R chart is added to the EWMA chart to monitor the residuals and detect shifts in the process variability. The control statistics monitored in the R chart is $R_j = \max_i(e_{ij}) - \min_i(e_{ij})$, in which $e_{ij}$ is the regression residual in the $i$th observation of the $j$th sample. The control limits for R chart are

$$\text{LCD} = \sigma(d_2 - Ld_3) \quad \text{and} \quad \text{UCD} = \sigma(d_2 + Ld_3), \tag{44}$$

where $L(> 0)$ is a constant. The values of $d_2$ and $d_3$ are commonly used constants that relate the range and standard deviation. These values are given Montgomery [88] for different values of $n$. Profile monitoring is not the same as traditional quality control monitoring, as here we are monitoring a function of several variables instead of traditional method of individual variable control.

## D.5 Conclusion

We outlined a proposal to develop the appropriate profile that represents brain activities in terms of one or more explanatory variables. We proposed methodology to monitor this profile and provide one step ahead forecast of brain activity based on the current value of the profile response. We also outlined the procedures to improve the forecasting ability of the proposed monitoring methodology.

# E Andriy Olenko: Independent component analysis for functional MRI

A central problem in statistics and signal processing, is finding a suitable representation of the data, by means of a suitable transformation. It is important for subsequent analysis of the data, whether it be pattern recognition, data compression, de-noising, visualisation or anything else, that the

data is represented in a manner that facilitates the analysis, and adequately represents the phenomenon being examined.

Independent component analysis (ICA) is a statistical and computational technique for revealing hidden features/structure that underlie sets of random variables, measurements, or signals [99]. As an alternative to hypothesis driven analytical techniques, ICA has been applied to fMRI data as an exploratory data analysis technique in order to find independently distributed spatial patterns that depict source processes in the data [100, 101, 102, 104].

Independent component analysis (ICA) defines a generative model for the observed multivariate data, which is typically given as a large database of samples. In the model, the data variables are assumed to be linear mixtures of some unknown latent variables, and the mixing system is also unknown. The latent variables are assumed to be non-gaussian and mutually independent, and they are called the independent components of the observed data. These independent components, also called sources or factors, are found by ICA. In many cases, the measurements are given as a set of parallel signals or time series; the term blind source separation is often used to characterise the information recovery aspect of ICA.

## E.1 The essence of ICA

Let us denote by $\mathbf{x}$ an $m$-dimensional random variable; the problem is then to find a function $\mathbf{f}$ so that the $n$-dimensional transform $\mathbf{s} = (s_1, s_2, \ldots, s_n)$ defined by

$$\mathbf{s} = \mathbf{f}(\mathbf{x})$$

has some desirable properties. In most cases, the representation is sought as a linear transform of the observed variables

$$\mathbf{s} = \mathbf{W}\mathbf{x}\,,$$

where $\mathbf{W}$ is a matrix to be determined. Using linear transformations makes the problem computationally and conceptually simpler, and facilitates the

interpretation of the results. Much of the ICA methodology can be extended to non-linear situations.

Independent component analysis (ICA) of the random vector $\mathbf{x}$ consists of finding a linear transform $\mathbf{s} = \mathbf{W}\mathbf{x}$ so that the components $s_i$ are as independent as possible, in the sense of maximizing some function/functional $F(s_1, \ldots, s_n)$ that measures independence. It follows from this definition that ICA has a regularisation aspect [101, 105], which, in part, explains its potential to exhibit robust behaviour.

The basic goal of ICA is to find a transformation in which the components are statistically as independent from each other as possible. Independent component analysis ICA is applied, for example, for blind source separation, in which the observed values of $\mathbf{x}$ correspond to a realisation of an $m$-dimensional discrete time signal $\mathbf{x}(t)$, $t = 1, 2, \ldots$. Then the components are called source signals, which are usually either original, uncorrupted signals or noise sources. Often such sources are statistically independent from each other, and thus the signals are recovered from linear mixtures by finding a transformation in which the transformed signals are as independent as possible, as in ICA. The use of ICA for feature extraction is motivated by results in neurosciences that suggest that the similar principle of redundancy reduction explains some aspects of the early processing of sensory data by the brain [102].

In the linear model for brain activation, the total brain activity $X(t, v)$ is assumed to be a linear superposition of the different ongoing brain activity patterns:

$$X(t, v) = \sum_{l=1}^{L} M_l(t) S_l(v),$$

where the $S_l(v)$ correspond to the brain activity patterns, and the mixing matrix $M$ gives the corresponding time courses. Matrix $M$ plays role of $W^{-1}$. In the simplest case

$$S_l(v) = \begin{cases} 1, & \text{if } v \in A_l\,, \\ 0, & \text{if } v \notin A_l\,, \end{cases}$$

where $A_l$ is some brain activity volumetric region of voxels.

So the sets $A_l$ show regions with different brain activities. The functions $M_l(t)$ provide us with information on specific changes in each region over time [102]. For the implementation of ICA, some of the issues that must be taken into consideration include:

- How should the contrast function $F(s_1, \dots, s_n)$ be chosen and validated?
- To what extent are the sets $A_l$ different for various contrast functions given in ICA literature (likelihood, entropy, mutual information, Kullback Leibler divergence, etc.)?

## E.2 Simultaneous EEG and fMRI

The use of joint EEG–fMRI measurements in brain activity research is a growing and promising field, with great potential to expand our understanding of epilepsy. Once the timing of the events has been determined from EEG, we compare it with time courses from ICA results. Knowing the timing of the spikes or original time series from EEG and the time series components $M_l(t)$ from ICA allows us to examine the fMRI signal to find $M_l(t)$ highly correlated with EEG time series. Then corresponding sets $A_l$ are regions of abnormal activity.

We let $Y(t)$ denote EEG recording over time. Then to chose volumetric regions of voxels $A_l$, where abnormal activity occurs, we select $l$ that maximises some function

$$G(Y(t), M_l(t)),$$

that measures similarities of EEG time series and time courses for different brain areas obtained from ICA where the simplest choice of $G$ is a correlation function.

For the implementation of ICA for the analysis of joint EEG–fMRI data, some of the issues that must be taken into consideration include:

- How should the similarity function $G(Y(t), M_l(t))$ be chosen and validated?
- Will results of this two stage algorithm be quite different from results of classical one stage methods which search a region of abnormal activity voxel by voxel?

# F Robert S. Anderssen: Synchronisation and the Kuramoto model

As is clear from the plots of EEG recordings of epileptic events/seizures, such as shown in Figure 1, the rapid onset of the highly oscillatory phases can be viewed as occurring through some major synchronisation activity within the brain. There is strong agreement that this is representative of the brain activity occurring prior to, at and during a seizure [39]. However, in modelling such synchronisation, the appropriateness of the Kuramoto model [118] has not been explicitly examined. This model has been indirectly linked with epilepsy and mentioned as an example of a complex network which synchronises.

The role of this appendix is to examine the extent to which the Kuramoto model represents a basis for modelling the synchronisation associated with epilepsy, and also determine the extent to which this model might provide insight about the nature of the synchronisation occurring. This discussion has been organised in the following manner. The phenomenon of synchronisation is discussed in Section F.1. The Kuramoto model, in an elementary form, is introduced in Section F.2 along with the concept of order parameter. Its appropriateness, relevance and utility for enhancing understanding of the synchronisation of brain activity prior to, at and during epileptic events/seizures are examined in Section F.3.

## F.1 The phenomenon of synchronisation

The phenomenon of synchronisation, closely related to the concepts of *'constructive interference'* and *'resonance'*, is a naturally occurring phenomenon. The first recorded observation appears to be that of Huygens in a letter dated February 27, 1665 [106]. Synchronisation is both a biological and a physicochemical phenomenon. As well as clocks, the physicochemical examples include lasers [107] and chemical waves [118]. Biologically, it is the mechanism that controls the beating of the heart with the synchronisation of the signalling coming from the heart's pacemaker (the sinoatrial (sinus) node) [108, 109]. Synchronisation is believe to be the process responsible for epileptic events and seizures [110] and has been utilised to model their dynamics [111, 112, 39].

As highlighted by a number of researchers [113, 67, 114], it was Winfree [115] who, in order to explain the observed behaviour of populations of biological oscillators, formulated a model consisting of a system of nearly identical and coupled limit cycle oscillators. Winfree [115] went on to prove that the system behaved incoherently or synchronised depending on the degree of coupling; namely, incoherent when the coupling was small compared with the spread of the frequencies of the oscillators, partial synchronisation when the coupling exceeded a threshold and fully locked phase and amplitude coupling for strong coupling, as illustrated by Strogatz [113, Figure 2].

Acebron et al. [114] gave a lucid discussion of the Kuramoto model as a simple paradigm for the study of synchronisation. The importance of having simple models is reflected in the following comment by Velazquez [110] *"a lesson for those who think that simple, naive models have little practical use in real life"* and discussed from an industrial mathematics perspective by de Hoog [116].

As outlined in the next section, it was Kuramoto [118] who formalised mathematically the observations of Winfree [115] in a form that yielded a mathematical framework in which to successfully study synchronisation. In addition, he proposed a simple and exactly solvable model of collective synchronisation

which highlighted explicitly the intuitive observations for Winfree [115] and thereby validated the appropriateness of his general mathematical model.

## F.2 The Kuramoto model

As already mentioned in Section 2, Kuramoto [118] formulated his model in order to place the observations and modelling of Winfree [115] on a more formal and general footing. Strogatz [117] gave an insightful discussion of the mathematics of the Kuramoto model. Because of its utility and appropriateness in modelling, for example, lasers, heart beat and brain activity, it is often cited as an example of a methodology for exploring complex networks [113].

For $N$ oscillators, the general form of the model proposed by Kuramoto [118], with $t$ denoting time, is

$$\dot{\theta}_j(t) = \omega_j + \sum_{i=1}^{N} \Gamma_{ji}(\theta_i - \theta_j), \quad \theta_j = \theta_j(t), \quad \dot{\theta}_j = \frac{d\theta_j}{dt}, \quad j = 1, \ldots, N, \tag{45}$$

where $\theta_j$ and $\omega_j$ denote, respectively, the phase and frequency of oscillator $j$ with the function $\Gamma_{ij}(\theta_j - \theta_i)$ defining the nature of the coupling occurring between oscillators $i$ and $j$.

The interesting special case of equally weighted, all-in-all, purely sinusoidal coupling, for which Kuramoto [118] gave an analytic solution, is

$$\dot{\theta}_j(t) = \omega_j + \frac{K}{N} \sum_{i=1}^{N} \sin(\theta_i - \theta_j), \quad j = 1, \ldots, N. \tag{46}$$

As explained by Strogatz [117], for highlighting the nature of the synchronisation implicit in this model, Kuramoto introduced the concept of an order parameter to characterise the degree of the synchronisation ( *"the collective*

*rhythm"* of the population of oscillators) occurring. The complex order parameter takes the form

$$r(t)\exp(i\psi(t)) = \frac{1}{N}\sum_{j=1}^{N}\exp(i\theta_j) \tag{47}$$

with $r(t)$ and $\psi(t)$ tracking the phase coherence and average phase of the population.

For his simple model (46), Kuramoto [118], using the order parameter definition, was able to rewrite, after some algebra, it in the following more compact (mean-field) form

$$\dot{\theta}_j(t) = \omega_j + Kr(t)\sin(\psi - \theta_j), \qquad j = 1, \ldots, N\,. \tag{48}$$

Even though the oscillators are interacting, this equation shows that the coupling is through the order parameter's phase coherence $r$ and the average phase $\psi$. It follows from (48) that, as the time $t$ progresses with synchronisation occurring, the phases $\theta_j$ are pulled towards $\psi$ rather than each other and the strength of the coupling is $Kr$.

## F.3 The Kuramoto model and epilepsy

The Kuramoto model, as discussed above, is now playing an increasing role in the modelling of neuronal activity [119, 120, 121]. However, the model's appropriateness as a model for the study of epilepsy remains an open question. The current emphasis on the study of epilepsy is focussed on techniques for the recovery of information jointly from EEG and fMRI data, with independent component analysis (ICA) receiving considerable attention [101, 104].

Various modelling aspects have been pursued but with only an indirect connection to the Kuramoto model. Kim et al. [112, 111, 39] used delay differential equations in their study of the evolution, spreading and suppression dynamics of epilepsy. Kim et al. [39] made a passing comment about *"Kuramato type*

*all-in-all coupling"* without specifically citing a publication by Kuramoto. However, they do cite papers related to Parkinson's disease where the Kuramoto model is specifically mentioned. Interestingly, in brain activity studies, the Kuramoto model is playing a quite important role in the study of desynchronisation in the context of pulse based desynchronisation techniques for the treatment of Parkinson's disease [103, 122, 123]. However, such investigations give no insight about the nature of the initiation of the synchronisation in either epilepsy or Parkinson's disease.

Kuramoto [119] examined collective synchronisation of pulse coupled oscillators and excitable units, where the concept of *"all-in-all mutual connection"* is introduced. This has relevance for neuronal modelling, because the neuronal interaction and communication is a pulsative interaction process.

As explained by Cumin and Unsworth [67] and others, from a brain activity perspective, the weakness of the simple Kuramoto model of Equation (45) is that it assumes that the coupling between each pair of oscillators contributing to the synchronisation are all the same. Clearly, as Cumin and Unsworth proposed, for the modelling of the synchronisation in brain activity, an appropriate generalisation of the Kuramoto model takes the form

$$\dot{\theta}_j(t) = \omega_j + \frac{1}{N}\sum_{i=1}^{N} K_{ij}(t)\sin(\theta_i - \theta_j), \quad j = 1, \ldots, N, \tag{49}$$

where the different levels of coupling between oscillators are not the same and change with the progression of the time $t$. The clear advantage of this model is that the synchronisation can be modelled over the whole brain by setting $K_{ij}(t)$ to be zero for the times when the coupling between the $i$th and $j$th oscillators is zero. Interestingly, through the introduction of an explicit dependence on the time $t$ into the coupling function $\Gamma_{ij}(\theta_i - \theta_j)$, the Cumin and Unsworth generalisation is also a generalisation of the original mean-field model of Kuramoto [118]. Cumin and Unsworth [67] performed extensive computational analysis of a coupled four component model to assess the utility of the generalisation.

A number of researchers examined the utility of the Cumin Unsworth generalisation for the modelling of neuronal activity. The utility of the generalisation is acknowledged by Velazquez et al. [124], who suggest its application to earlier work on desynchronisation [122]. It is explicitly exploited by Lin and Lin [125] and Ghosh et al. [126], who used the generalisation to study neuronal synchronisation in the brain. A connection to the circadian rhythm was made by Granada et al. [59].

However, Velazquez [110] highlighted the importance and usefulness of mathematical modelling in helping to generate a deeper understanding of biological processes, and, in particular, brain activity synchronisation applied to practical situations such as epilepsy and Parkinson's disease. Velazquez [110] mentioned that due care must be exercised in the interpretation of the results flowing from such endeavours. As Velasquez says, it is important to reflect on

> how certain or uncertain it is to conceptualise brain function based on these theoretical frameworks, if the physiological and experimental constraints are not as accurate as the models prescribe.

A particular concern that he raises is the

> uses and abuses of mathematical formalisms and techniques that are being applied in brain research, particularly the current trend of using dynamical system theory to unravel the global, collective dynamics of brain activity.

# References

[1] C. M. Michel, G. Thut, S. Morand, A. Khateb, A. J. Pegna, R. Grave de Peralta, S. Gonzalez, M. Seeck and T. Landis, Electric source imaging of human brain functions, *Brain Res. Rev.*, **36**(2–3), 2001, 108–118. doi:10.1016/S0165-0173(01)00086-8 M40

[2] S. Ogawa, R. S. Menon, S. G. Kim and K. Ugurbil, On the characteristics of functional magnetic resonance imaging of the brain, *Annu. Rev. Bioph. Biom.*, **27**, 1998, 447–474. doi:10.1146/annurev.biophys.27.1.447 M40, M50

[3] C. D. Binnie and H. Stefan, Modern electroencephalography: its role in epilepsy management, *Clin. Neurophysiol.*, **110**(10), 1999, 1671–1697. doi:10.1016/S1388-2457(99)00125-X M40

[4] J. X. Tao, A. Ray, S. Hawes-Ebersole and J. S. Ebersole, Intracranial EEG substrates of scalp EEG interictal spikes, *Epilepsia*, **46**(5), 2005, 669–76. doi:10.1111/j.1528-1167.2005.11404.x M41, M48

[5] S. Ogawa, D. W. Tank, R. Menon, J. M. Ellermann, S. G. Kim, H. Merkle and K. Ugurbil, Intrinsic signal changes accompanying sensory stimulation: Functional brain mapping with magnetic resonance imaging, *P. Natl. Acad. Sci.* USA, **89**(13), 1992, 5951–5955. doi:10.1073/pnas.89.13.5951 M41, M50

[6] J. Engel Jr., Report of the ILAE classification core group, *Epilepsia*, **47**(9), 2006, 1558–1568. doi:10.1111/j.1528-1167.2006.00215.x M43, M62

[7] L. Lemieux, A. Salek-Haddadi, O. Josephs, P. Allen, N. Toms, C. Scott, K. Krakow, R. Turner and D. R. Fish, Event-related fMRI with simultaneous and continuous EEG: description of the method and initial case report, *NeuroImage*, **14**(3), 2001, 780–7. doi:10.1006/nimg.2001.0853 M41

[8] P. Federico, D. F. Abbott, R. S. Briellmann, A. S. Harvey and G. D. Jackson, Functional MRI of the pre-ictal state, *Brain*, **128**(8), 2005, 1811-7. doi:10.1093/brain/awh533 M44, M64

[9] C. S. Hawco, A. P. Bagshaw, Y. Lu, F. Dubeau and J. Gotman, BOLD changes occur prior to epileptic spikes seen on scalp EEG, *NeuroImage*, **35**(4), 2007, 1450–1458. doi:10.1016/j.neuroimage.2006.12.042 M44

[10] F. Moeller, H. R. Siebner, S. Wolff, H. Muhle, R. Boor, O. Granert, O. Jansen, U. Stephani and M. Siniatchkin, Changes in activity of striato-thalamo-cortical network precede generalized spike wave discharges, *NeuroImage*, **39**(4), 2008, 1839–1849. doi:10.1016/j.neuroimage.2007.10.058 M44

[11] V. Osharina, E. Ponchel, A. Aarabi, R. Grebe and F. Wallois, Local haemodynamic changes preceding interictal spikes: A simultaneous electrocorticography (ECoG) and near-infrared spectroscopy (NIRS) analysis in rats, *NeuroImage*, **50**(2), 2010, 600–607. doi:10.1016/j.neuroimage.2010.01.009 M44

[12] R. S. Fisher, W. Boas, W. Blume, C. Elger, P. Genton, P. Lee and J. Engel, Epileptic seizures and epilepsy: Definitions proposed by the international league against epilepsy (ILAE) and the international bureau for epilepsy (IBE), *Epilepsia*, **46**(4), 2005, 470–472. doi:10.1111/j.0013-9580.2005.66104.x M46, M62

[13] H. Berger, Electroencephalogram in humans, *Arch. Psychiat. Nerven.*, **87**, 1929, 527–570. M47

[14] C. M. Michel, M. M. Murray, G. Lantz, S. Gonzalez, L. Spinelli and R. G. de Peralta, EEG source imaging, *Clin. Neurophysiol.*, **115**(10), 2004, 2195–2222. doi:10.1016/j.clinph.2004.06.001 M49

[15] P. L. Nunez and R. B. Silberstein, On the relationship of synaptic activity to macroscopic measurements: Does co-registration of EEG with fMRI make sense?, *Brain Topogr.*, **13**(2), 2000, 79–96. doi:10.1023/A:1026683200895 M49

[16] S. Ogawa, T. M. Lee, A. R. Kay and D. W. Tank, Brain magnetic resonance imaging with contrast dependent on blood oxygenation, *P. Natl. Acad. Sci.* USA, **87**(24), 1990, 9868–9872. doi:10.1073/pnas.87.24.9868 M50, M52

[17] J. S. Gati, R. S. Menon, K. Ugurbil and B. K. Rutt, Experimental determination of the BOLD field strength dependence in vessels and tissue, *Magn. Reson. Med.*, **38**(2), 1997, 296–302. doi:10.1002/mrm.1910380220 M50

[18] P. A. Bandettini, E. C. Wong, R. S. Hinks, R. S. Tikofsky and J. S. Hyde, Time course EPI of human brain function during task activation, *Magn. Reson. Med.*, **25**(2), 1992, 390–397. M50

[19] K. K. Kwong, J. W. Belliveau, D. A. Chesler, I. E. Goldberg, R. M. Weisskoff, B. P. Poncelet, D. N. Kennedy, B. E. Hoppelm, M. S. Cohen and R. Turner, Dynamic magnetic resonance imaging of human brain activity during primary sensory stimulation, *P. Natl. Acad. Sci.* USA, **89**(12), 1992, 5675–5679. doi:10.1073/pnas.89.12.5675 M50

[20] J. Frahm, K. D. Merboldt and W. Hnicke, Functional MRI of human brain activation at high spatial resolution, *Magn. Reson. Med.*, **29**(1), 1993, 139–144. M50, M51

[21] P. A. Bandettini, A. Jesmanowicz, E. C. Wong and J. S. Hyde, Processing strategies for time-course data sets in functional MRI of the human brain, *Magn. Reson. Med.*, **30**(2), 1993, 161–173. M50, M51

[22] K. J. Friston, P. Jezzard and R. Turner, Analysis of functional MRI time-series, *Hum. Brain Mapp.*, **1**(2), 1994, 153–171. M50, M51

[23] B. Biswal, F. Z. Yetkin, V. M. Haughton and J. S. Hyde, Functional connectivity in the motor cortex of resting human brain using echo-planar MRI, *Mag. Reson. Med.*, **34**(4), 1995, 537–541. doi:10.1002/mrm.1910340409 M50

[24] K. J. Friston, J. Ashburner, C. D. Frith, J. Poline, J. D. Heather and R. S. J. Frackowiak, Spatial registration and normalization of images, *Hum. Brain Mapp.*, **3**(3), 1995, 165–189. M51

[25] K. J. Friston, S. Williams, R. Howard, R. S. Frackowiak and R. Turner, Movement-related effects in fMRI time-series, *Magn. Reson. Med.*, **35**(3), 1996, 346–355. M51

[26] G. H. Glover, T. Q. Li and D. Ress, Image-based method for retrospective correction of physiological motion effects in fMRI: Retroicor, *Magn. Reson. Med.*, **44**(1), 2000, 162–167. doi:10.1002/1522-2594(200007)44:13.0.CO;2-E M51

[27] K. J. Friston, O. Josephs, G. Rees and R. Turner, Nonlinear event-related responses in fMRI, *Magn. Reson. Med.*, **39**(1), 1998, 41–52. doi:10.1002/mrm.1910390109 M51

[28] K. Ugurbil, L. Toth and D. Kim, How accurate is magnetic resonance imaging of brain function?, *Trends Neurosci.*, **26**(2), 2003, 108–114. doi:10.1016/S0166-2236(02)00039-5 M52

[29] D. S. Kim, I. Ronen, C. Olman, S. G. Kim, K. Ugurbil and L. J. Toth, Spatial relationship between neuronal activity and BOLD functional MRI, *NeuroImage*, **21**(3), 2004, 876–885. doi:10.1016/j.neuroimage.2003.10.018 M52

[30] A. Connelly, G. D. Jackson, R. S. Frackowiak, J. W. Belliveau, F. Vargha-Khadem and D. G. Gadian, Functional mapping of activated human primary cortex with a clinical MR imaging system, *Radiology*, **188**(1), 1993, 125–130. M52

[31] L. Allison, Hidden Markov Models, *Technical Report*, School of Computer and Software Engineering, Monash University, 2000. M54

[32] R. J. Elliott, L. Aggoun and J.B. Moore, Hidden Markov Models: Estimation and Control, *Appl. Math.-Czech.*, 2004. M54, M75, M76, M77, M79

[33] B. Bhavnagri, *Discontinuities of plane functions projected from a surface with methods for finding these*, Technical Report, 2009. M55, M82, M83, M85

[34] B. Bhavnagri, *Computer Vision using Shape Spaces*, Technical Report,1996, University of Adelaide. M55, M83

[35] B. Bhavnagri, A method for representing shape based on an equivalence relation on polygons, *Pattern Recogn.*, **27**(2), 1994, 247–260. doi:10.1016/0031-3203(94)90057-4 M55, M86

[36] D. F. Abbott, A. B. Waites, A. S. Harvey and G. D. Jackson, Exploring epileptic seizure onset with fMRI, *NeuroImage*, **36(S1)** (344TH-PM), 2007. M56

[37] M. C. Mackey and L. Glass, Oscillation and chaos in physiological control systems, *Science*, **197**, 1977, 287–289. M57

[38] S. H. Strogatz, *SYNC - The Emerging Science of Spontaneous Order*, Theia, New York, 2003. M57

[39] J. W. Kim, J. A. Roberts and P. A. Robinson, Dynamics of epileptic seizures: Evolution, spreading, and suppression, *J. Theor. Biol.*, **257**(4), 2009, 527–532. doi:10.1016/j.jtbi.2008.12.009 M57, M98, M99, M101

[40] Y. Kuramoto, T. Aoyagi, I. Nishikawa, T. Chawanya T and K. Okuda, Neural network model carrying phase information with application to collective dynamics, *J. Theor. Phys.*, **87**(5), 1992, 1119–1126.

[41] V. B. Mountcastle, The columnar organization of the neocortex, *Brain*, **120**(4), 1997, 701. doi:10.1093/brain/120.4.701 M61

[42] F. L. Silva, W. Blanes, S. N. Kalitzin, J. Parra, P. Suffczynski and D. N. Velis, Epilepsies as dynamical diseases of brain systems: Basic models of the transition between normal and epileptic activity, *Epilepsia*, **44**(12), 2003, 72–83. M63, M67

[43] F. H. Lopes da Silva, W. Blanes, S. N. Kalitzin, J. Parra, P. Suffczynski and D. N. Velis, Dynamical diseases of brain systems:

different routes to epileptic seizures, IEEE *T. Bio-Med. Eng.*, **50**(5), 2003, 540. M63, M67

[44] L.D. Iasemidis, Epileptic seizure prediction and control, IEEE *T. Bio-Med. Eng.*, **50**(5), 2003, 549–558. M64

[45] L. D. Iasemidis, D. S. Shiau, W. Chaovalitwongse, J. C. Sackellares, P. M. Pardalos, J. C. Principe, P. R. Carney, A. Prasad, B. Veeramani, and K. Tsakalis, Adaptive epileptic seizure prediction system, IEEE *T. Bio-Med. Eng.*, **50**(5), 2003, 616–627. M64

[46] K. Lehnertz, F. Mormann, T. Kreuz, R.G. Andrzejak, C. Rieke, P. David and C. E. Elger, Seizure prediction by nonlinear EEG analysis, IEEE *Eng. Med. Biol.*, **22**(1), 2003, 57–63. doi:10.1109/MEMB.2003.1191451 M64

[47] K. Lehnertz, R. G. Andrzejak, J. Arnhold, T. Kreuz, F. Mormann, C. Rieke, G. Widman and C. E. Elger, Nonlinear EEG analysis in epilepsy: Its possible use for interictal focus localization, seizure anticipation, and prevention, *J. Clin. Neurophysiol.*, **18**(3), 2001, 209. M64

[48] B. Litt and K. Lehnertz, Seizure prediction and the preseizure period, *Curr. Opin. Neurol.*, **15**(2), 2002, 173. doi:10.1097/00019052-200204000-00008 M64

[49] B. Litt and J. Echauz, Prediction of epileptic seizures, *Lancet Neurol.*, **1**(1), 2002, 22–30. doi:10.1016/S1474-4422(02)00003-0 M64

[50] M. Mäkiranta, J. Ruohonen, K. Suominen, J. Niinimäki, E. Sonkajärvi, V. Kiviniemi, T. Seppänen, S. Alahuhta, V. Jäntti and O. Tervonen, BOLD signal increase preceeds EEG spike activity–a dynamic penicillin induced focal epilepsy in deep anesthesia, *NeuroImage*, **27**(4), 2005, 715–724. doi:10.1016/j.neuroimage.2005.05.025 M64

[51] K. Lehnertz, F. Mormann, H. Osterhage, A. Müller, J. Prusseit, A. Chernihovskyi, M. Staniek, D. Krug, S. Bialonski and C. E. Elger,

State-of-the-art of seizure prediction, *J. Clin. Neurophysiol.*, **24**(2), 2007, 147. doi:10.1097/WNP.0b013e3180336f16 M64, M72

[52] F. Mormann, T. Kreuz, C. Rieke, R. G. Andrzejak, A. Kraskov, P. David, C. E. Elger and K. Lehnertz, On the predictability of epileptic seizures, *Clin. Neurophysiol.*, **116**(3), 2005, 569–587. doi:10.1016/j.clinph.2004.08.025 M66

[53] F. Mormann, R. G. Andrzejak, C. E. Elger and K. Lehnertz, Seizure prediction: the long and winding road, *Brain*, **130**(2), 2007, 314–333. doi:10.1093/brain/awl241 M64, M80

[54] Z. Rogowski, I. Gath and E. Bental, On the prediction of epileptic seizures, *Biol. Cybern.*, **42**(1), 1981, 9–15. M64

[55] Y. Salant, I. Gath, O. Henriksen, Prediction of epileptic seizures from two-channel EEG, *Med. Biol. Eng. Comput.*, **36**(5), 1998, 549–556. doi:10.1007/BF02524422 M64

[56] J. Gotman and D.J. Koffler, Interictal spiking increases after seizures but does not after decrease in medication, *Evoked Potential*, **72**(1), 1989, 7–15. M65

[57] J. Gotman and M. G. Marciani, Electroencephalographic spiking activity, drug levels, and seizure occurence in epileptic patients, *Ann. Neurol.*, **17**(6), 1985, 59–603. M65

[58] A. Katz, D. A. Marks, G. McCarthy and S. S. Spencer, Does interictal spiking change prior to seizures?, *Electroen. Clin. Neuro.*, **79**(2), 1991, 153–156. M65

[59] A. Granada, R. M. Hennig, B. Ronacher, A. Kramer and H. Herzel, Phase Response Curves: Elucidating the dynamics of couples oscillators, *Method Enzymol.*, **454**(A), 2009, 1–27. doi:10.1016/S0076-6879(08)03801-9 doi:10.1016/S0076-6879(08)03801-9 M103

[60] H. Kantz and T. Schreiber, *Nonlinear time series analysis*, 2004, Cambridge Univ Press. M65

[61] M. V. L. Bennett and R. S Zukin, Electrical coupling and neuronal synchronization in the mammalian brain, *Neuron*, **41**(4), 2004, 495–511. doi:10.1016/S0896-6273(04)00043-1 M65

[62] L.D. Iasemidis, J. Chris Sackellares, H. P. Zaveri and W. J. Williams, Phase space topography and the Lyapunov exponent of electrocorticograms in partial seizures, *Brain Topogr.*, **2**(3), 1990, 187–201. doi:10.1007/BF01140588 M65

[63] M. Le Van Quyen, J. Martinerie, V. Navarro, M. Baulac and F. J. Varela, Characterizing neurodynamic changes before seizures, *J. Clin. Neurophysiol.*, **18**(3), 2001, 191. M65

[64] J. Martinerie, C. Adam, M. Le Van Quyen, M. Baulac, S. Clemenceau, B. Renault and F. J. Varela, Epileptic seizures can be anticipated by non-linear analysis, *Nat. Med.*, **4**(10), 1998, 1173–1176. doi:10.1038/2667 M65

[65] A. Pikovsky, M. Rosenblum, J. Kurths and R. C. Hilborn, Synchronization: A universal concept in nonlinear science, *Amer. J. Phys.*, **70**, 2002, 655. M66

[66] H. R. Wilson and J. D. Cowan, Excitatory and inhibitory interactions in localized populations of model neurons, *Biophys. J.*, **12**(1), 1972, 1–24. M69

[67] D. Cumin and C. P. Unsworth, Generalising the Kuramoto model for the study of neuronal synchronisation in the brain, *Physica D*, **226**(2), 2007, 181–196. doi:10.1016/j.physd.2006.12.004 M70, M99, M102

[68] F. K. Skinner, H. Bazzazi and S. A. Campbell, Two-cell to N-cell heterogeneous, inhibitory networks: Precise linking of multistable and coherent properties, *J. Comput. Neurosci.*, **18**(3), 2005, 343–352. doi:10.1007/s10827-005-0331-1 M70

[69] W. W. Lytton, Computer modelling of epilepsy, *Nat. Rev. Neurosci.*, **9**(8), 2008, 626–637. doi:10.1038/nrn2416 M71

[70] R. D. Traub, A. Bibbig, F. E. N. LeBeau, E. H. Buhl and M. A. Whittington, Cellular mechanisms of neuronal population oscillations in the hippocampus in vitro, *Ann. Rev.*, 2004. M71

[71] R. D. Traub, A. Draguhn, M. A. Whittington, T. Baldeweg, A. Bibbig, E. H. Buhl and D. Schmitz, Axonal gap junctions between principal neurons: A novel source of network oscillations, and perhaps epileptogenesis., *Rev. Neuroscience*, **13**(1), 2002, 1. doi:10.1146/annurev.neuro.27.070203.144303 M71

[72] M. Scheffer, J. Bascompte, W. A. Brock, V. Brovkin, S. R. Carpenter, V. Dakos, H. Held, E. H. van Nes, M. Rietkerk and G. Sugihara, Early-warning signals for critical transitions, *Nature*, **461**(7260), 2009, 53–59. doi:10.1038/nature08227 M73, M79, M87

[73] K. Murphy, *A Brief Introduction to Graphical Models and Bayesian Networks*, 2008, http://www.cs.ubc.ca/murphyk/Bayes/bnintro.html. M73

[74] R. C. Bradley, An elementary treatment of the Radon Nikodym Derivative, *Am. Math. Mon.*, **96**(5), 1989, 437–440. M77

[75] S. Bretschneider, Estimating forecast variance with exponential smoothing, *Int. J. Forecasting*, **2**, 1986, 349–355. M80

[76] R. A. J. Masterton, D. F. Abbott, S. W. Flemin and G. D. Jackson, Measurement and reduction of motion and ballistocardiogram artefacts from simultaneous EEG and fMRI recordings, *NeuroImage*, **37**,(1), 2007, 202-211. doi:10.1016/j.neuroimage.2007.02.060 M83

[77] M. Moosmann, V. H. Schnfelder, K. Specht, R. Scheeringa, H. Nordby amd K. Hugdahl, Realignment parameter-informed artefact correction for simultaneous EEG-fMRI recordings, *NeuroImage*, **45**(4), 2009, 1144-1150. doi:10.1016/j.neuroimage.2009.01.024 M83

[78] A. Connes and M. A. Rieffel, *Lect. Notes. Math*, 1994, Academic Press, San Diego, California. M87

[79] A. L. Carey and J. Phillips, Algebras almost commuting with Clifford algebras in a II$\infty$ factor, *K-Theory*, **4**(5), 1991, 445–478. M87

[80] A. L. Carey and D. E. Evans, Algebras Almost Commuting with Clifford Algebras, *J. Funct. Anal.*, **88**,(2), 1990, 279–298. doi:10.1007/BF00533214 M87

[81] J. D. Williams, J. B. Brich, W. H. Woodall and N. M. Ferry, Statistical monitoring of heteroscedastic does-response profiles from high-throughput screening, *J. Agric. Biol. Envir. S.*, **12**(2), 2007, 216–235. doi:10.1198/108571107X197779 M88

[82] M. A. Mahmoud and W. H. Woodall, Phase I analysis of linear profiles with calibration applications, *Technometrics*, **46**, 2004, 277–391. doi:10.1198/004017004000000455 M88, M90

[83] J. O. Ramsay and B. W. Silverman, *Functional Data Analysis*, 3rd Edition, 1997, Springer–Verlag, New York. M88

[84] M. A. Mahmoud, P. A. Parker, W. H. Woodall and D. M. Hawkins, A change point method for linear profile data, *Qual. Reliab. Eng. Int.*, **23**, 2007, 247–268. doi:10.1002/qre.788 M88

[85] M. M. Gardner and J. C. Lu, Equipment Fault detection using Spatial Signatures, IEEE *T. Compon. Pack. C*, **20**, 1997, 295–304. doi:10.1109/3476.650961 M88

[86] J. Jin and J. Shi, Automatic feature extraction of waveform signals for in-process diagnostic performance improvement, *J. Intell. Manuf.*, **12**(3), 2001, 257–268. M88

[87] J. Jin and J. Shi, Feature preserving data compression of stamping tonnage information using wavelet, *Technometrics*, **41**(4), 1999, 327–339. M88

[88] D. C. Montgomery, *Introduction to Statistical Quality Control*, 5th edition, 2005, John Wiley and Sons, New York. M88, M92, M94

[89] K. J. Worsley, C. Liao, J. Aston, V. Petre, G. Duncan, F. Orales and A. Evans, A general statistical analysis for fMRI data, *NeuroImage*, **15**(1), 2002, 1–15. doi:10.1006/nimg.2001.0933 M88

[90] C. R. Genoves, A Bayesian time course model for functional magnetic resonance imaging data, *J. Am. Stat. Assoc.*, **95**, 2000, 691–719. M88

[91] N. Lange and S.L. Zeger, Non-Linear Fourier time series analysis for human brain mapping by functional magnetic resonance imaging, *J. R. Stat. Soc.*, **14**, 1997, 1–29. M88

[92] P. L. Purden, V. Solo, R. M. Weisskoff and E. Brown, Locally regularized spatiotemporal modelling and model comparison for functional MRI, *NeuroImage*, **14**, 2001, 912–923. doi:10.1006/nimg.2001.0870 M88

[93] K. J. Worsley, Detecting activation in fMRI data, *Stat. Methods Med. Res.*, **12**(5), 2003, 401–418. doi:10.1191/0962280203sm340ra M88

[94] M. Neter, H. Kutner, C. J. Nachtsheim and W. Wasserman, *Applied Linear Regression Models*, 3rd Edition, 1996, IrwinS, Chicago. M90

[95] L. Kang and S.L. Albin, On-line monitoring when the process yields a linear profile, *J. Qual. Technol.*, **32**, 2000, 418–426. M90, M91

[96] C. Aou and F. Tsung, Monitoring profiles based on nonparametric regression methods, *J. Am. Stat. Assoc.*, **4**, 2008, 1512–526. doi:10.1198/004017008000000433 M91

[97] A. Azzalini and A. W. Bowman, On the use of nonparametric regression for checking linear relationship, *J. R. Stat. Soc.*, 1993, 549–557. M91

[98] O. Mestek, J. Pavlik and M. Suchanek, Multivariate control charts for calibration curves, *Fresen. J. Anal. Chem.*, **350**, 1994, 344–351. doi:10.1007/BF00325603 M91

[99] A. Hyvarinen, Fast and robust fixed-point algorithms for independent component analysis, IEEE *T. Neural Networ.*, **10**(3), 1999, 626–634. doi:10.1109/72.761722 M95

[100] C. F. Beckmann and S. A. Smith, Probabilistic independent component analysis for functional magnetic resonance imaging, IEEE *T. Med. Imaging*, **23**(2), 2004, 137–152. doi:10.1109/TMI.2003.822821 M95

[101] V. D. Calhoun, T. Adali, M. C. Stevens, K. A. Kiehl and J. J. Pekar, Semi-blind ICA of fMRI: a method for utilizing hypothesis-derived time courses in a spatial ICA analysis, *NeuroImage*, **25**(2), 2005, 527–538. doi:10.1016/j.neuroimage.2004.12.012 M95, M96, M101

[102] I. Daubechies, E. Roussos, S. Takerkart, M. Benharrosh, C. Golden, K. D'Ardenne, W. Richter, J. D. Cohen and J. Haxby, Independent component analysis for brain fMRI does not select for independence, *P. Natl. Acad. Sci.* USA, **106**(26), 2009. doi:10.1073/pnas.0903525106 M95, M96, M97

[103] K. Dolan, M. Majtanik and P. A. Tass, Phase resetting and transient desynchronization in networks of globally coupled phase oscillators with inertia, *Physica D*, **211**(1-2), 2005, 128–138. doi:10.1016/j.physd.2005.08.009 M102

[104] T. Eichele, V. D. Calhoun, and S. Debener, Mining EEG-fMRI using independent component analysis, *Int. J. Psychophysiol.*, **73**(1), 2009, 53–61. doi:10.1016/j.ijpsycho.2008.12.018 M95, M101

[105] P. Bai, H. Shen, X. Huang and Y. Truong, A supervised singular value decomposition for independent component analysis of fMRI, *Stat. Sinica*, **18**(4), 2008, 1233-1252. M96

[106] M. Bennett, M. F. Schatz, H. Rockwood and K. Wiesenfeld, Huygens's clocks, *P. Roy. Soc. Lond. A Mat.*, **458**(2019), 2002, 563–579. doi:10.1098/rspa.2001.0888 M99

[107] M. K. S. Yeung and S. H. Strogatz, Time delay in the Kuramoto model of coupled oscillators, *Phys. Rev.*, **82**(3), 1999, 648–651. M99

[108] A. T. Winfree, *The Geometry of Biological Time*, 1990, Springer Verlag, New York. M99

[109] K. Okuda and Y. Kuramoto, Mutual entrainment between populations of coupled oscillators, *Prog. Theo. Phys.*, **86**(6), 1991, 1159–1176. M99

[110] J. L. P. Velazquez, Brain, behaviour and mathematics: Are we using the right approaches?, *Physica D*, **212**(3-4), 2005, 161–182. doi:10.1016/j.physd.2005.10.005 M99, M103

[111] J. W. Kim and P. A. Robinson, Controlling limit-cycle behaviors of brain activity, *Physical Review E*, **77**(5), 2008. doi:10.1103/PhysRevE.77.051914 M99, M101

[112] J. W. Kim and P. A. Robinson, Compact dynamical model of brain activity, *Phys. Rev. E*, **75**(3), 2007. doi:10.1103/PhysRevE.75.031907 M99, M101

[113] S. H. Strogatz, Exploring complex networks, *Nature*, **410**(6825), 2001, 268–276. M99, M100

[114] J. A. Acebron, L. L. Bonilla, C. J. P. Vicente, F. Ritort and R. Spigler, The Kuramoto model: A simple paradigm for synchronization phenomena, *Rev. Mod. Phys.*, **77**(1), 2005, 137–185. doi:10.1103/RevModPhys.77.137 M99

[115] A. T. Winfree, Biological rhythms and behavior of populations of couple oscillators, *J. Theor. Biol.*, **16**(1), 1967, 15. M99, M100

[116] F. R. de Hoog, Why are simple models often appropriate in industrial mathematics?, In R. S. Anderssen, R. Braddock and L. Newham,

*Proceedings of the 18th World* IMACS/MODSIM *Congress, Cairns, July 13-17*, 2009, 23–36. doi:978-0-9758400-7-8 M99

[117] S. H. Strogatz, From Kuramoto to Crawford: Exploring the onset of synchronization in populations of coupled oscillators, *Physica D*, **143**(1-4), 2000, 1–20. M100

[118] Y. Kuramoto, *Chemical Oscillations, Waves and Turbulence*, 1984, Springer Verlag, Berlin. M57, M98, M99, M100, M101, M102

[119] Y. Kuramoto, Collective synchronization of pulse-coupled oscillators and excitable units, *Physica D*, **50**(1), 1991, 15–30. M101, M102

[120] S. K. Han, C. Kurrer and Y. Kuramoto, Dephasing and bursting in coupled neural oscillators, *Phys. Rev. Lett.*, **75**(17), 1995, 3190–3193. doi:10.1103/PhysRevLett.75.3190 M101

[121] T. D. Frank, A. Daffertshofer, C. E. Peper, P. J. Beek and H. Haken, Towards a comprehensive theory of brain activity: Coupled oscillator systems under external forces, *Physica D*, **144**(1-2), 2000, 62–86. M101

[122] M. Majtanik, K. Dolan and P. A. Tass, Desynchronization in networks of globally coupled neurons with dendritic dynamics, *J. Bio. Phys.*, **32**(3-4), 2006, 307–333. doi:10.1007/s10867-006-9018-8 M102, M103

[123] M. Moazami-Goudarzi, J. Sarnthein, L. Michels, R. Moukhtieva and D. Jeanmonod, Enhanced frontal low and high frequency power and synchronization in the resting EEG of parkinsonian patients, *NeuroImage*, **41**(3), 2008, 985–997. doi:10.1016/j.neuroimage.2008.03.032 M102

[124] J. L. P. Velazquez, R. F. Galan, L. G. Dominguez, Y. Leshchenko, S. Lo, J. Belkas and R. G. Erra. Phase response curves in the characterization of epileptiform activity, *Phys. Rev. E*, **76**(6), 2007. doi:10.1103/PhysRevE.76.061912 M103

[125] C. Lin and M. Lin, The mathematical research for the Kuramoto model of the describing neuronal synchrony in the brain, *Commun. Nonlinear Sci.*, **14**(8), 2009, 3258–3260. doi:10.1016/j.cnsns.2009.01.007 M103

[126] A. Ghosh, D. Roy amd V. K. Jirsa, Simple model for bursting dynamics of neurons, *Phys. Rev. E*, **80**(4), 2009. doi:10.1103/PhysRevE.80.041930 M103

## Author addresses

1. **J. M. Dunn**, Dept. Maths and Geospatial Sciences, RMIT University, Melbourne, AUSTRALIA
   mailto:jessica.dunn@rmit.edu.au
2. **R. A. J. Masterton**, Brain Research Institute, Melbourne, AUSTRALIA
3. **D. F. Abbott**, Brain Research Institute, Melbourne, AUSTRALIA
4. **R. S. Anderssen**, CSIRO Mathematics, Infomatics and Statistics, Canberra, AUSTRALIA